



3RD ANNUAL DEPARTMENT OF RADIATION ONCOLOGY RESEARCH SYMPOSIUM

Friday, March 28, 2025 | 11:30am-5:45pm

SMC Campus Center, Rooms 208 and 210

Featuring

Poster Session

Keynote Speaker

Elana J. Fertig, PhD, FAIMBE

Director, Institute for Genome Sciences

University of Maryland Baltimore



Guest Speaker

Giuliano Scarcelli, PhD

Associate Professor, Dept. of Bioengineering & Biophysics Program

University of Maryland



Research Presentations

Award Presentation

Awards given out for top 3 best posters and top 3 best talks

Reception



Decipher® Prostate
Genomic Classifier



Welcome to the 2025 Department of Radiation Oncology Symposium!

AGENDA

LOCATION:

SMC Campus Center
2nd Floor
621 W Lombard St
Baltimore, MD 21201

TIME	INFO	LOCATION
11:00am-11:30am	Check-in & Registration	
11:30am-12:45pm	Working Lunch/Poster Session Attendees will be provided with a lunch box to pick-up	Room 210
12:45pm-1:00pm	Formal Welcome, Dept Research Overview: William F. Regine, MD, FACR, FASTRO, FACRO Isadore and Fannie Schneider Foxman Chair & Distinguished Professor Department of Radiation Oncology Senior Associate Dean for Clinical Affairs University of Maryland School of Medicine Thank Sponsors, Keynote Introduction: France Carrier, PhD Director of Tumor Biology Department of Radiation Oncology University of Maryland School of Medicine	Room 208
1:00pm-1:30pm	Keynote Speaker Elana J. Fertig, PhD, FAIMBE Director of Institute for Genome Sciences University of Maryland School of Medicine	Room 208
1:30pm-2:30pm	Biology Session Shirin Azarbarzin, PhD Triet Nguyen, BA Yang Song, PhD Zachery Keepers, BS	Room 208
2:30pm-2:45pm	Break	
2:45pm-2:50pm	Guest Speaker Introduction: Amit Sawant, PhD Vice Chair of Medical Physics Department of Radiation Oncology University of Maryland School of Medicine	Room 208

2:50pm-3:20pm	Guest Speaker: Giuliano Scarcelli, PhD Associate Professor Department of Bioengineering and Biophysics Program University of Maryland	Room 208
3:20pm-4:20pm	Physics Session Aman Sangal, PhD Dario Rodrigues, PhD Gulakhshan Hamad, PhD Stewart Becker, PhD	Room 208
4:20pm-5:20pm	Clinical Session Austin Thompson, MD Jarey Wang, MD Matthew Brown, MD Xiaolei Shi, MD, PhD	Room 208
5:20pm-5:30pm	Research Grant Awardee Matthew Brown, PhD PGY-4, Co-Chief Resident Department of Radiation Oncology University of Maryland School of Medicine	Room 208
5:30pm-5:35pm	Closing Comments France Carrier, PhD	Room 208
5:35pm-5:45pm	Award Presentation Photos (Everyone, Speakers, Winners, Etc.)	Room 208
5:45pm	Reception	Outside Room 208/210



Follow us on X @UMarylandRadOnc and tweet
today's event at #DeptRadOncSymposium

Keynote Speaker



Elana J. Fertig, PhD, FAIMBE

Dr. Fertig is a Professor of Medicine and Director of the Institute for Genome Sciences at University of Maryland. She advances a new predictive medicine paradigm for oncology by converging systems biology with translational technology development. Her wet lab develops time course models of therapeutic resistance and single cell technology development for analysis of clinical biospecimens. Her computational methods blend mathematical modeling and artificial intelligence to determine the biomarkers and molecular mechanisms of therapeutic resistance and disease progression from multi-platform genomics data. Prior to entering the field of computational cancer biology, Dr Fertig was a NASA research fellow in numerical weather prediction. Dr. Fertig's research is featured in over numerous peer-reviewed publications, R/Bioconductor packages, and competitive funding portfolio as PI and co-I. Her computational biology research has had broad applicability to the analysis of clinical biospecimens, developmental biology, and neuroscience.

Guest Speaker



Giuliano Scarcelli, PhD

Giuliano Scarcelli is an associate professor at the University of Maryland in the Bioengineering department and the Biophysics program. Giuliano obtained his PhD in quantum optics with a EU funded graduate fellowship between the University of Bari, Italy and UMBC, USA. Giuliano then was at the Wellman Center for Photomedicine of Harvard Medical School for eight years, first as a postdoc in Prof. Yun's Lab, then as an instructor and assistant professor. He joined the University of Maryland in 2015. Giuliano has been the recipient of several awards such as the "Exceptional by example" award for outstanding PhD studies, the Tosteson Postdoctoral Fellowship at Harvard, the Human Frontier Science Program Young Investigator Award, the NIH Quantitative Career Award, the NSF CAREER award and "Teaching excellence" awards from both Harvard University and University of Maryland.

Research Presentations

Biology Session Speakers

Shirin Azarbarzin, PhD

Developing a syngeneic minipigs pancreatic cancer model as a suitable large animal model for FLASH radiation therapy.



Shirin Azarbarzin holds a Ph.D. in Biology-Molecular Genetics, with a focus on miRNA replacement therapy in cancer cells, targeting PD-L1, cytokine secretion in T-cells, and the underlying signaling pathways in breast cancer. She has been a postdoctoral fellow at the University of Maryland's Marlene and Stewart Greenebaum Comprehensive Cancer Center in Baltimore, USA, where her research has focused on targeted therapies and drug resistance in head and neck squamous cell carcinoma (HNSCC), particularly investigating signaling pathways such as PI3K/AKT/mTOR.

Currently, she is working in Dr. Carrier's lab, studying the RNA-binding protein hnRNP A18, a key regulator of protein translation that targets specific signature motifs in the 3' UTR of transcripts in cancer cells. Her research also involves investigating small-molecule inhibitors targeting hnRNP A18. She has extensive expertise in cell and molecular biology and is actively involved in developing new reagents for cancer research, including pig cancer cell lines.

Triet Nguyen, BA

TWIST1 Associates with Resistance to Treatment and Twist1 Drives Tumor Progression in vivo for Small Cell Lung Cancer



Triet Nguyen is a 5th year PhD candidate in the Tran lab at the University of Maryland, Baltimore. After obtaining his B.A. in Biochemistry and Molecular Biology (BMB) from Franklin & Marshall College, Triet began his PhD training in the BMB program at the Johns Hopkins Bloomberg School of Public Health. For his thesis research, Triet investigates the roles the EMT program plays in small cell lung cancer development, dissemination, and acquisition of therapy resistance.

Yang Song, PhD

A digital pathology multimodal artificial intelligence algorithm is associated with pro-metastatic genomic pathways in oligometastatic prostate cancer



Dr. Song is a Senior Bioinformatics Analyst at the Institute for Genome Sciences at the University of Maryland, Baltimore. She earned a Ph.D. in Molecular Cell Biology and an M.S. in Statistics simultaneously, laying the foundation for her career in genomic research and big data analysis. With over 10 years of experience, she specializes in next-generation sequencing, biomarker discovery, functional genomics, bulk and single-cell omics, metagenomics, and meta-transcriptomics analysis. Dr. Song has contributed to numerous studies on prostate cancer, small-cell lung cancer, head and neck cancer, organ transplantation, hearing loss, and infectious diseases.

Zachery Keepers, BS

Synergy with decitabine expands the utility of talazoparib: a novel therapeutic strategy for BRCA-proficient pancreatic cancer



Zachery graduated from the University of Maryland, College Park, with a degree in Bioengineering and is currently a third-year medical student at the University of Maryland School of Medicine. Since participating in the Radiation Oncology Summer Fellowship in 2023, he has worked on several clinical, translational, and basic science projects in the department. He is excited by interacting with and connecting researchers in these respective domains. Today, he will be presenting a collaborative effort spanning multiple departments that aims to test a novel combination treatment for pancreatic cancer.

Physics Session Speakers

Aman Sangal, PhD

Simulating realistic digital phantoms for virtual clinical trials in radiology and radiation oncology using a deep-learning based conditional Denoising Diffusion Probabilistic Model (c-DDPM)



Dr. Aman Sangal earned his PhD in experimental high-energy physics from the University of Cincinnati, collaborating with the Belle experiment at KEK, Japan, where he explored particle matter interactions, developing expertise in radiation physics, detector operations, computing skills, big data analysis, machine learning, and Monte Carlo simulations. He also received the esteemed Ozaki Exchange Fellowship from the Brookhaven National Laboratory (BNL) during his doctoral studies, facilitating advanced research in Japan.

Currently, Dr. Sangal serves as a postdoctoral researcher in Dr. Lei Ren's lab, leading projects at the intersection of AI and radiotherapy. His broad focus lies in developing

AI based digital phantoms to improve imaging and treatment optimization in radiotherapy. A key project involves the development of the RT-XCAT phantom, using a deep learning-based diffusion model trained on CT data from liver cancer patients to generate realistic patient-specific artificial CT images.

Dr. Sangal's long-term goal is to transition into clinical medical physics, applying his expertise in fundamental physics, AI and imaging to improve patient treatment outcomes and contribute to the advancement of medical physics in clinical settings.

Dario Rodrigues, PhD

Numerical feasibility of delivering deep hyperthermia to lateral tumors opposite to metallic hip implants



Dr. Dario Rodrigues is an Assistant Professor of Radiation Oncology, lead hyperthermia physicist and Director of the Hyperthermia Therapy Practice School at the University of Maryland School of Medicine (Maryland, USA). Dr. Rodrigues obtained his PhD in Biomedical Engineering from a collaboration between the NOVA University Lisbon (Portugal) and Duke University (North Carolina, USA). As a medical physicist, Dr. Rodrigues performs adjuvant hyperthermia treatments that are combined with chemo- or radiotherapy to treat cancer patients. He also implements treatment planning, thermal dosimetry, and quality assurance of clinical microwave/radiofrequency (MW/RF) hyperthermia equipment. In support of his clinical activities, his research involves the development of improved MW/RF- and

magnetic nanoparticle-based applicators for applying heat to tissue as well as new hyperthermia treatment planning strategies to improve thermal dose delivery. This research is accomplished with a combination of theoretical modeling, engineering development, and equipment performance evaluation with phantom, animal, and human patient subjects. Dr. Rodrigues is also a councilor of engineering/physical sciences for the Society for Thermal Medicine (STM), chair of the Thermal Medicine Standards Committee hosted by the American Society of Mechanical Engineers (ASME), and a member of the Technical Committee of the European Society for Hyperthermic Oncology (ESHO).

Gulakhshan Hamad, PhD

COMBINING PROTON FLASH AND SPATIALLY FRACTIONATED RADIOTHERAPY – EXPERIMENTAL AND SIMULATION BASED DOSIMETRIC CHARACTERIZATION



Gulakhshan Hamad is a postdoctoral fellow at the Maryland University School of Medicine, where her research focuses on combining ultra-high dose rate (UHDR) proton therapy and spatially fractionated radiotherapy (SFRT) - cutting-edge approaches designed to improve tumor control while minimizing damage to healthy tissues. With a strong background in nuclear physics and radiation applications, her work is dedicated to enhancing the precision and effectiveness of modern cancer treatments.

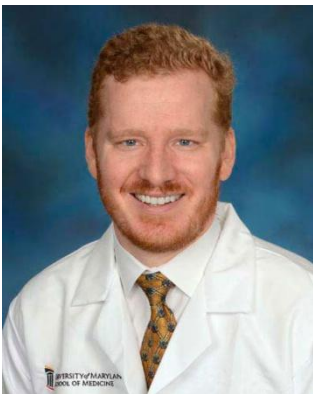
She earned her master's degree in Nuclear Physics from Ohio University, where her research centered on the three-dimensional structure of the nucleon—a fundamental inquiry that helps answer key questions about the origin of nucleon spin and the charge and density distributions within the nucleon. She then pursued my Ph.D. in Nuclear Physics at Ohio University, focusing on nuclear reactions relevant to nuclear astrophysics and nuclear medicine, bridging the gap between fundamental science and practical applications.

Before her current role, she served as a postdoctoral researcher at Johnson Pharmaceuticals of J&J and NIST (Associate), where she contributed to the development of activity standards for the radionuclide ^{225}Ac , a crucial component in targeted radiotherapy.

Beyond her professional pursuits, she enjoys hiking and climbing. She also enjoys building Gundam models, a hobby that reflects her love for engineering, precision, and creative problem-solving.

Stewart Becker, PhD

The GammaPod reduces organ-at-risk dose and creates more conformal plans compared to VMAT when delivering accelerated partial breast irradiation (APBI)



Dr. Becker is a board certified Medical Physicist. He received his PhD from University of Wisconsin-Madison in Medical Physics. Dr. Becker joined us, in 2014, from the NYU Langone Medical Center where he was a physicist in the Department of Radiation Oncology and scholar at the NYU Institute for Innovations in Medical Education.

Dr. Becker is an internationally known expert in the GammaPod (a stereotactic radiosurgery technique for the breast) and has traveled the world assisting new centers in the installation of their GammaPods.

Clinical Session Speakers

Austin Thompson, MD

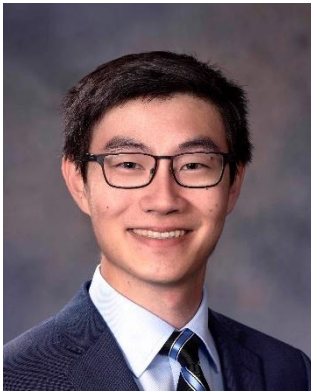
The Effect of Residing in a Food-Insecure Area on Locally Advanced Breast Cancer Survival



Austin Thompson is a PGY-3 radiation oncology resident at the University of Maryland Department of Radiation Oncology. During medical school, he researched patterns of failure in gynecologic malignancies across different radiation treatment modalities and helped run a free healthcare clinic serving uninsured members of the regional Latino community. In residency, his research has focused on reirradiation outcomes, disparities in cancer treatment outcomes, and the use of interstitial hyperthermia with brachytherapy.

Jarey Wang, MD, PhD

Proteomic profiling of oligometastatic castration-sensitive prostate cancer treated with stereotactic ablative radiotherapy



Jarey Wang is currently a PGY-4 Radiation Oncology resident at Johns Hopkins. He received his MD/PhD at Baylor College of Medicine and has a background in both bioinformatics and bench research. He currently conducts research in oligometastatic prostate cancer with Drs. Phuoc Tran and Ana Kiess, and he has a specific interest in "omics" data and clinical biomarkers.

Matthew Brown, MD

The Genomic Landscape of Human Papillomavirus Positive Early Stage Oropharyngeal Carcinoma



Dr. Matthew Brown is Chief Resident of Radiation Oncology in the medical residency here at the University of Maryland, where he has trained for 3 years in the clinical practice of radiation oncology. Dr. Brown earned his medical degree from the University of Alabama at Birmingham (UAB), where he published multiple articles on the use of SRS for brain metastases, and has since developed a keen interest in integrating innovative technologies with radiation oncology. During his research year, Dr. Brown has led work in enhancing hybrid applicator brachytherapy for the treatment of advanced cervical cancer by utilizing machine learning algorithms. He has also worked to contribute to the limited genomic landscape of early stage p16+ oropharyngeal cancer. Both of which will be presented today. This past year, he was accepted into the AACR/ASCO Clinical Trials Workshop, often colloquially referred to as "Vail", for the development of a prospective phase II randomized trial comparing the acute toxicity of proton therapy and photon therapy in patients with gynecologic malignancies. The first of its kind, this protocol is completed and

planned to open here at UMMC pending funding. Additionally, Dr. Brown serves on the American College of Radiation Oncology (ACRO) resident committee as the Chair of Communications. In addition to his clinical and research work, Dr. Brown is dedicated to education and mentorship and has recently worked to help modify to the format of didactics in the residency program.

Xiaolei Shi, MD, PhD

Prognostic validation of six androgen production, uptake, and conversion genes (APUC-6) in the ECOG-ACRIN E3805 CHAARTED prostate cancer trial



Dr. Xiaolei Shi earned her medical degree from Harbin Medical University in China and completed her PhD in cancer biology at UT Southwestern Medical Center. She then pursued her Internal Medicine residency at the University of Minnesota. Currently, she is a second-year Medical Oncology fellow at the University of Maryland Medical Center (UMMC) and T32 Training Fellow in Cancer Biology under the mentorship of Dr. Phuoc Tran.

Award Presentation

Awards given out for top 3 best posters and top 3 best talks:

1st Winner - \$500 each
2nd Winner - \$250 each
3rd Winner - \$100 each

***A HUGE THANK YOU to our wonderful sponsors for
their generous support of this event!***

Decipher® Prostate Genomic Classifier



"T'EMPUS



Follow us on X @UMarylandRadOnc and tweet
today's event at #DeptRadOncSymposium

#	Name	Abstract Title	Principal Investigator(s)
1	Arezoo Modiri, PhD	A Novel Imaging Biomarker for the Early Detection of Cardiotoxicity	Arezoo Modiri, PhD
2	Weiguang Yao, PhD	Proton range-based patient setup	Weiguang Yao, PhD
3	Adeniyi Olabumuyi, MBBS	Evaluating the Correlation Between Genomic Classifier and Digital Pathology-Based Multi-Modal AI Biomarkers in Localized Prostate Cancer	Phuoc T. Tran, MD, PhD
4	Aaron Chan, BS	Investigating the Impact of ZNFX1 in Non-Small Cell Lung Cancer Tumorigenesis	Phuoc T. Tran, MD, PhD Feyruz V. Rassool, PhD
5	Travis Hoover, MD	Definitive radiation therapy for early-stage cancer of the hypopharynx and supraglottis	Matthew J. Ferris, MD
13	Hajar Moradmand, PhD	Graph-Based Radiomics: Enhancing Stability and Reproducibility in AI-Driven Multi-Institutional Head and Neck Cancer Analysis	Lei Ren, PhD
15	Hem D Shukla, PhD	Clinical validation of the role of Caveolin-1 in radiation and chemotherapy resistance in lung cancer	Hem D Shukla, PhD
17	Vijay Sharma, PhD	Assessment of a Novel Snout-Mounted Imaging System for Dose Depth Monitoring	Lei Ren, PhD
19	Danielle Waters, MLAS	Investigating Genetic Mechanisms of Tumorigenesis in Non-Small Cell Lung Cancer Transgenic Mice using Tumor Barcoding with Barcode Deep-Sequencing	Phuoc T. Tran, MD, PhD
20	Nrusingh Biswal, PhD	Treatment plan LET validation using measured integral depth dose for proton therapy	Nrusingh C. Biswal, PhD Weiguang Yao, PhD
21	Muhammad Ajmal Khan, PhD	Twist1 Overexpression Models an Aggressive Subtype of Pancreatic Ductal Adenocarcinoma in vivo	Phuoc T. Tran, MD, PhD
22	Yankun Lang, PhD	Enhancing Image Quality in Acoustic Imaging Using the Segment Anything Model (SAM)	Lei Ren, PhD
23	Kaushlendra Tripathi, PhD	DNMTi in combination with PARPi inhibits aberrant WNT/Beta-catenin and Tenascin C pathway signaling, decreasing cancer stemness and metastasis in triple-negative breast cancer	Feyruz V. Rassool, PhD
24	Hem D Shukla, PhD	3-Bromopyruvate in combination with radiation inhibits pancreatic tumor growth by stalling glycolysis, and dismantling mitochondria in a syngeneic mouse model	Hem D Shukla, PhD

25	Dipanwita Dutta Chowdhury, MS	TNIK-induced chemoradiation resistance in small cell lung cancer	Phuoc T. Tran, MD, PhD
26	Jin Hee Chang, BS	Investigating the role of TNIK in the pathogenesis of lung squamous cell carcinoma	Phuoc T. Tran, MD, PhD
30	Noura Radwan, MD, MBA	Phase 2 randomized high-risk metachroNous oligometastatic prostate cancer with hiGh-risk mutations treated with meTastasiS directed therapy and niraparib/abiraterone acetate plus prednisone (KNIGHTS) trial	Jason Molitoris, MD, PhD Phuoc T. Tran, MD, PhD
31	Jie Zhang, PhD	Enhance Four-dimension Cone-beam Computed Tomography (4D-CBCT) From Sparse Views Using A Novel Deep Learning Model	Lei Ren, PhD
33	Robabeh Rahimi, PhD	Quantum-inspired genetic optimization tailored for patient scheduling in radiation oncology	Robabeh Rahimi, PhD
34	Robabeh Rahimi, PhD	First Demonstration of Prostate Radiotherapy Plan Optimization on an IBM Quantum Computer	Amit Sawant, PhD
35	Matthew Eason, BS	Pleckstrin Homology domains regulate PI3K/Akt to block breast cancer dissemination	Aikaterini Kontrogianni-Konstantopoulos, PhD
36	Apurva Singh, PhD	Prediction of metastasis-free survival in patients with prostate adenocarcinoma using primary tumor and lymph node radiomics from pre-treatment PSMA PET/CT scans.	Lei Ren, PhD
38	Charlyn Gomez, BS	Centering Black Voices: Factors Influencing a Cancer Patient's Decision to Join a Clinical Trial - Study Update	Melissa Ana Liriano Vyfhuis, MD, PhD
39	Alex Allen, MD	Clinical Toxicity Profiles of Neoadjuvant Volumetric Modulated Arc Radiotherapy and Proton Beam Radiotherapy for Soft Tissue Sarcoma: A Single-Institution Retrospective Analysis	William Regine, MD, FACR, FASTRO, FACRO

Title:

A Novel Imaging Biomarker for the Early Detection of Cardiotoxicity

Author list (not sure about the order):

Arezoo Modiri¹, Ivan Vogelius², Amit Sawant¹, Jens Petersen²

¹ Department of Radiation Oncology, University of Maryland, School of Medicine

² Department of Oncology, University of Copenhagen, Rigshospitalet, Copenhagen, Denmark

Purpose: In cardiology, the pericardium sac is considered a fast responder to cardiac injuries and any decline in pericardium health can potentially be an early biomarker of a later cardiac event. We hypothesize that changes in pericardium due to radiation could also be used as early biomarkers for late cardiotoxicity which is the second major cause of death after the cancer itself among thoracic cancer patients receiving radiotherapy (RT).

Methods: We performed a retrospective study of 522 patients, 234 males and 288 females, age: 28 to 93 (median 68), treated with chemo-RT for small cell and non-small-cell lung cancer in Rigshospitalet from 2009 to 2020. Anonymized dosimetric, demographic and health history information were studied. Median of mean heart dose was 2.8 Gy (max: 36.4Gy). The whole heart and its 4-millimeter outmost layer (pericardium sac) were contoured on the standard-of-care baseline (Pre-RT) and 5-to-8-month post-RT follow-up CT scans that were deformably registered on the baseline CT images. Histogram of Hounsfield unit (HU) changes in pericardium sac voxels was studied. We calibrated for the effect of contrast enhancement using 41 patient cases who had no contrast in neither baseline nor follow-up.

Results: Voxel-based HU change histogram had a skewed distribution with a mean and skewness that were correlated with mean doses to both pericardium sac (Spearman correlation factor [SCF] ± 0.7 ($P < 0.05$)) and the whole heart (SCF ± 0.6 ($P < 0.05$)). Histogram skewness was also correlated with patient sex (SCF 0.6 ($P < 0.05$)) while the histogram mean was correlated with post-RT cardiovascular events (SCF 0.6 ($P < 0.05$)). Interestingly, pericardial dose response remained pronounced when each tissue composition was studied separately. On average, voxels with HU ranges associated with fibrosis and calcification increased in follow-up CTs consistently with the increase in dose.

Tissue-composition-based dose response	Mean normalized HU change from baseline to 6-month followup in the related voxels (%)				
	Voxel dose in pericardium sac				
Tissue type on baseline CT	<1Gy	1-5Gy	5-10Gy	10-20Gy	>20Gy
Fat (-500<HU<-30)	-1.65	-1.35	-1.33	-1.12	-1.12
Effusion (-5<HU< 30)	-0.19	-0.17	-0.26	-0.28	-0.30
Normal tissue (31<HU<60)	0.10	0.07	0.02	-0.05	-0.02
Fibrosis (65<HU<120)	0.18	0.21	0.19	0.22	0.32
Calcification (500>HU>130)	0.15	0.24	0.30	0.44	0.78

Conclusion: Pericardium composition distribution has a dose-dependent change at 6 months post-RT. These changes are detectable on standard of care CT scans and are potential early markers of late cardiotoxicity.

Impact: “Despite a reported 10 million deaths from cancer, there are an estimated 16.9 million cancer survivors in the US, with the number projected to increase to 22.2 million by 2030. Cardiovascular disease is the leading non-neoplastic cause of morbidity and mortality in survivors of thoracic cancers treated with radiotherapy and chemotherapy. This is an area of unmet research need, as little is known about clinical risk evaluation and the best population and modality for screening.”[1] Underdiagnosis in current practice due to limiting the screening benefit to symptomatic patients adversely affects cardiac care quality for cancer patients. Our study suggests an image-based early biomarker and has the potential to contribute to prospective cardiac care in radiation oncology.

Novelty: Abnormalities in pericardium sac have been associated with higher mortality risk [2] and assessing pericardium health has been recommended as a part of clinical practice for identifying patients at greater risk of developing cardiovascular diseases.[3] Here, we investigate preclinical pericardial abnormalities detectable on standard-of-care (SOC) images as novel early markers for late cardiac events.

Methods: Our original patient number was 1751 from which those with missing data were excluded. Several patients had multiple followup images with different scanners/reconstruction-kernels within our time frame of interest. To find the followup image best matching the baseline image in terms of reconstruction kernel and scanner, we calculated the average difference in voxel Hounsfield unit values between the baseline and followup image sets in an out-of-field region near the heart. The selected region was the part of a 5cm ring around the heart mask that had received no radiation dose (Figure 1). The follow-up scan selected was the one with the least difference in HU distribution in this region with the baseline CT. Using Plastimatch software, we deformable-registered follow-up images on baseline images. Totalsegmentator was used for contouring the heart. Four-millimeter outmost layer of the heart was taken as pericardium sac. Normalized changes for various tissue compositions were calculated using voxel Hounsfield units (HUs):

$$\text{Normalized HU Change} = \frac{\sum_{\vartheta \in S \& CT(\vartheta) \in HUbin} (followup HU(\vartheta) - baseline HU(\vartheta))}{\sum_{\vartheta \in S} (planning HU(\vartheta) + 1000)}$$

Mean dose to pericardium was <1Gy for 144 patients, 1-5Gy for 150, 5-10Gy for 98, 10-20 Gy for 92 and >20 Gy for 38 patients.

Key Results: Figure 2 shows voxel-based analysis results where dose to voxel is used to bin the voxels and follow their HU change using the above equation. The left panel has baseline CT values (starting points) on the x axis and the right panel has followup CT values (ending points) on the x axis. There was a detectable dose-response in pericardial HU distribution that correlated with various tissue compositions (fat, effusion, normal tissue, fibrosis and calcification). For instance, looking to the right panel, (1) the large peak on the positive y side moves to right from normal tissue HU range for the green curve to fibrosis and calcification HU ranges for the yellow and red curves as the dose increases, and (2) the smaller peak on the negative region of left side shows a decrease in fat HU region independent of radiation dose; this could be associated to overall weight/fat loss for most cancer patients under treatment.

References:

[1] Velusamy, R., et al., *Screening for Coronary Artery Disease in Cancer Survivors: JACC: CardioOncology State-of-the-Art Review*. JACC CardioOncol, 2023. **5**(1): p. 22. [2] Klein, A.L., et al., *Mortality and the Pericardial Sac: Are We Only Scratching the Surface?* J Am Coll Cardiol, 2020. **76**(22): p. 2632. [3] Tarsitano, M.G., et al., *Epicardial Adipose Tissue: A Novel Potential Imaging Marker of Comorbidities Caused by Chronic Inflammation*. Nutrients, 2022. **14**(14)

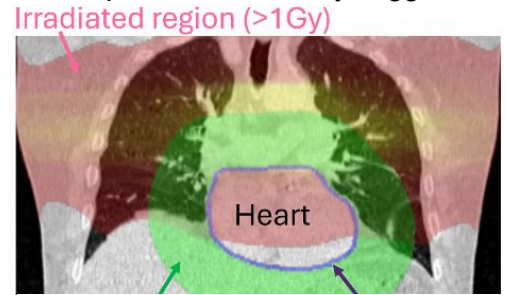


Fig.1. Heart and pericardium contours along with the $\leq 1\text{Gy}$ dose area around the heart.

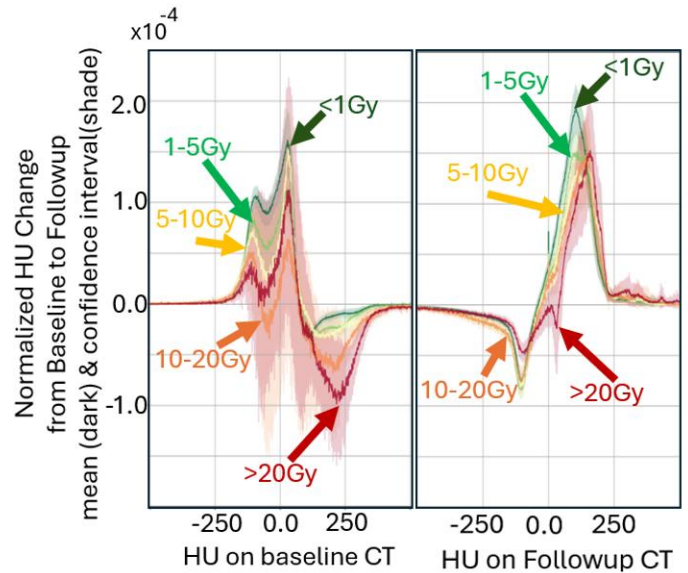


Fig.2. Normalized HU change using voxel dose for binning with respect to the baseline HU values (left panel) and the followup HU values (right panel).

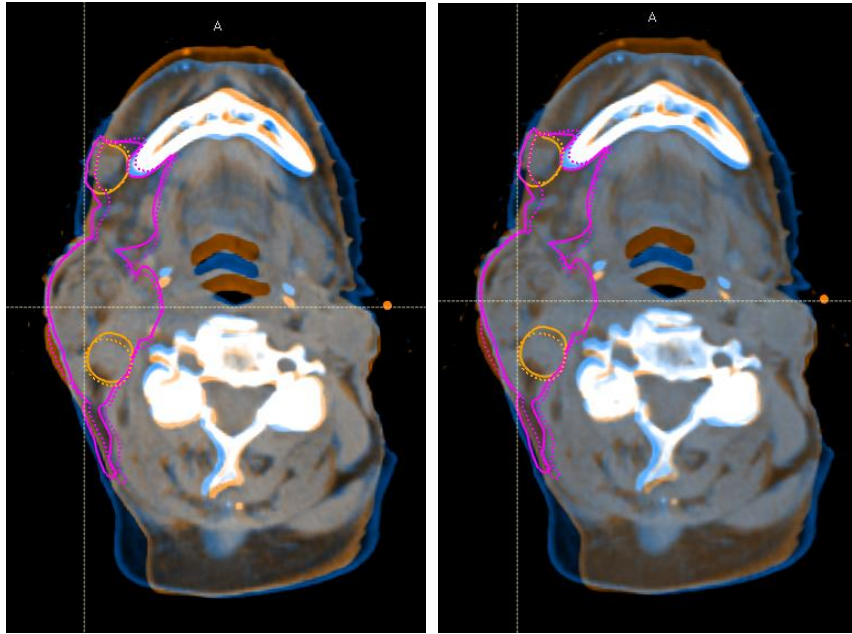
Proton range-based patient setup

Weiguang Yao

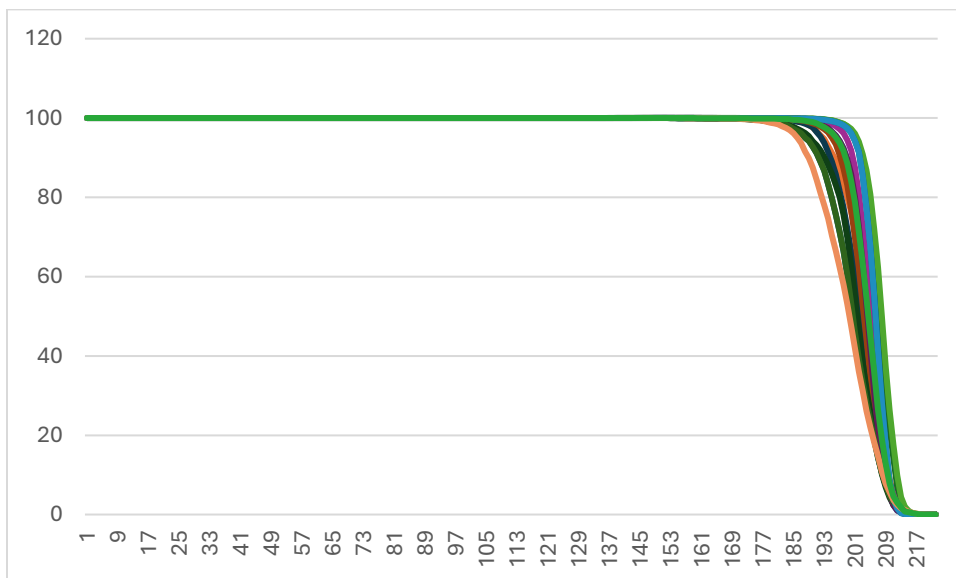
Purpose: For proton therapy, image guidance may not be sufficient for patient setup. This is because proton dose delivery is sensitive to the proton range, but our image guidance is not based on the range. In this study, we investigated the delivered dose to patients under image-guidance and range-based setups.

Methods and Materials: Two proton head-and-neck patients with QACTs and CBCTs were used. One patient had diseases on the right side and the other had diseases in the base of the tongue. A range-based registration algorithm was developed to register the QACTs and CBCTs to the planning CT. With the obtained range-based registration parameters (shifts and rotations), the normal procedures were performed to deform the target contours from the planning CT to QACTs and then the dose from the treatment plan to the QACTs was calculated in RayStation treatment planning system (TPS). The dose volume histogram (DVH) of the target from range-based registration was compared to the DVH from image-guidance registration. The image-guidance registration was performed by the dosimetrist during the QA plan evaluation. For CBCTs, range-based registration was done against the first day CBCT, i.e. the first day CBCT was used as the reference. The range-based and image-guidance registration parameters were applied to the planning CT to calculate the dose. Ideally, if there is no difference between these two registrations, the dose will be the same as the planned dose, and otherwise the dose will be different. The image-guidance registration was done by the therapist during patient setup.

Results: For the patient with diseases on the right side, the DVH in the QACTs was sensitive to the registration parameters. $D_{95}=87.7\%$ in the QACT (a replan was required due to the result of D_{95}), but $D_{95}=98.9\%$ in the QACT by extra shifts (3, -1, -1) mm in the lateral, AP and SI directions from the original image-guidance registration. The extra shifts were obtained by our range-based registration. The results from CBCTs showed that the average $D_{95}=92.8\%$. For the other patient, V_{100} was improved in a QACT from 91.8% to 95.0% by extra shifts (0, 1, 1) mm.



The figures above show the registration of the QACT to the planning CT by (left) image-guidance and (right) range-based registration. The difference in the registration parameters is 3 mm in lateral, 1 mm in AP and 1 mm in SI directions. Both registrations may be acceptable from the match of the images and the difference seems negligible, but the dose to the target is significantly different because beams tangential to the skin are used. The plan consists of 3 beams: 195, 320 and 350 degrees, where beams 195 and 350 are tangential to the skin.



The figure above shows the DVHs calculated from the planning CT, which is additionally shifted from the original image-guidance registration. The additional shifts were

determined by range-based registration for each CBCT. The maximum additional shifts were 3 mm in each direction.

Conclusion: Range-based registration can significantly improve proton dose delivery, especially for the cases where beams tangential to the skin are used.

Adeniyi A. Olabumuyi, Olivia G. Jordan, Jinhee Chang, Claudia Datnow-Martinez, Scott E. Delacroix, Daniel E. Spratt, Xiaolei Shi, Yang Liu, Elai Davicioni, Huei-Chung Huang, Meghan Tierney, Michael S. Kim, Samir P. Kanani, Zaker H. Rana, Jason K. Molitoris, Mark V. Mishra, Young Kwok, Philip Sutera, Matthew Deek, Phuoc T. Tran

Evaluating the Correlation Between Genomic Classifier and Digital Pathology-Based Multi-Modal AI Biomarkers in Localized Prostate Cancer

Purpose/Objectives

Prostate cancer is the second most common cancer in men, with 1 in 8 diagnosed in their lifetime. Risk stratification relies on T-stage, PSA, and Gleason score, while biomarker tests like Decipher Prostate Genomic Classifier (GC) and Artera Multi-Modal AI (MMAI) enhance prognostic accuracy. Both are validated for localized disease and provide risk information on clinical outcomes (e.g., distant metastasis, mortality) influencing decisions. MMAI can also predict short-term ADT (ST-ADT) benefit. The NRG GU010 trial uses GC to stratify unfavorable intermediate-risk (UIR) patients for treatment intensification. Whether GC and MMAI assess overlapping biology differently or offer complementary insights remains unclear. This study evaluates their correlation and association.

Materials/Methods

We conducted a retrospective single-institution study of localized prostate cancer patients who underwent GC and MMAI testing between May–December 2024. Demographics and clinical characteristics were summarized. GC scores were derived from RNA profiling per Decipher test (Veracyte, San Diego, CA). MMAI scores were generated from digitized H&E slides integrating image-based and clinical features per ArteraAI test (Artera, San Francisco, CA). Pearson's correlation assessed GC/MMAI score relationships, and cross-tabulation with percent agreement evaluated prognostic risk group association. GC-based ST-ADT classification (<0.4 , ≥ 0.4 per GU010) was compared with MMAI ST-ADT biomarker.

Results

A total of 76 patients [age: 54–83y, mean 68.9y; 52 (68%) White, 19 (25%) Black; 73 (96%) Non-Hispanic] were analyzed, with most classified as NCCN UIR [very low/low: 1 (1.3%), favorable intermediate: 20 (26.3%), UIR: 52 (68.4%), high: 2 (2.6%)]. GC and MMAI scores showed moderate correlation ($r = 0.487$, $p < 0.001$), increasing in UIR patients ($r = 0.533$, $p < 0.001$). Categorical risk groups were significantly associated ($p = 0.008$), with 43.6% of MMAI low-risk patients classified as GC low-risk and 66.7% of MMAI intermediate-risk patients as GC high-risk. No patients were MMAI high-risk. Overall agreement was 40% (30/75), and 36% (19/52) in UIR. Among GC ≥ 0.4 (GU010 darolutamide arm), 4.5% were MMAI ST-ADT positive. Among GC < 0.4 (GU010 ADT deintensification), 17.0% were MMAI ST-ADT positive (Table 1).

Conclusion

Decipher GC and Artera MMAI scores are modestly correlated, and categorical prognostic scores are not interchangeable. Given Artera ST-ADT MMAI positive tumors were nearly all GC

low risk, and almost all higher GC score patients were ST-ADT MMAI negative, further work is needed to understand the clinical implications of this observation in contemporary cohorts.

Table 1. Cross-tabulations between GC and MMAI

		Artera MMAI		
		Low	Int	High
Decipher GC	Low (<0.45)	24 (43.6%)	3 (13.4%)	0 (0.0%)
	Int (0.45-0.6)	15 (27.3%)	4 (19.0%)	0 (0.0%)
	High (>0.6)	16 (29.1%)	14 (66.7%)	0 (0.0%)
		Artera ST-ADT MMAI		
		Positive	Negative	
Decipher GC (GU 010 cutoffs)	< 0.4	9 (16.9%)	44 (83.1%)	
	≥0.4	1 (4.5%)	21 (95.5%)	

Investigating the Impact of ZNFX1 in Non-Small Cell Lung Cancer Tumorigenesis.

Authors:

Aaron Chan^{1,+}, Jinhee Chang¹, Danielle N. Waters¹, Elan Simms¹, Lora Stojanovic¹, Kaushlendra Tripathi¹, Triet Nguyen¹, Dipanwita Dutta Chowdhury¹, Hwai Wei Tseng¹, Muhammed Ajmal Khan¹, Audrey Lafargue^{1,#}, Phuoc T. Tran^{1,#}, Feyruz V. Rassool^{1,#}.

Affiliations:

¹Department of Radiation Oncology, Division of Translational Radiation Sciences, University of Maryland Baltimore, School of Medicine, Baltimore, MD, USA.

+Presenter.

#Corresponding authors: frassool@som.umaryland.edu; phuoc.tran@umm.edu; alafargue@som.umaryland.edu

Abstract:

Non-small cell lung cancer (NSCLC) accounts for more than 80% of all lung cancer diagnoses and is a major cause of cancer mortality. *KRAS* oncogene alterations (e.g. *KRAS*^{G12D} mutation) are among the most common gene alterations in NSCLC, and to this day are associated with nearly “undruggable” NSCLC disease. Recent studies have investigated the role of NFX1-type zinc finger-containing 1 protein (*Znfx1*) in ovarian cancer and determined that high *ZNFX1* expression correlates with increased overall survival in patients with advanced resistant ovarian cancer. Additionally, *ZNFX1* appeared to mediate treatment response, and knocking-out *ZNFX1* in vivo and in vitro enhanced tumorigenic programs and tumor growth, identifying *ZNFX1* as a tumor suppressor candidate. Interestingly, TCGA data revealed that *ZNFX1* might exhibit similar functions in NSCLC. To investigate whether *ZNFX1* loss contributes to tumorigenesis enhancement, we have generated a novel genetically engineered mouse model: Cas9-CR (*Cas9*; *CCSP-rtTA*; *tetO-KRas*^{G12D}), that allows inducible expression in lung epithelium of the *Kras*^{G12D} oncogene under Doxycycline treatment and the CRISPR-CAS9 knock-out of *Znfx1* by intra-tracheal instillation of lentiviral vector delivering *Znfx1* single-guide RNA to the lungs. Lung tissues will be analyzed (RNA and protein expressions analyses) to confirm *Znfx1* knock-out and *Kras*^{G12D} expression. Lung tumors development will be monitored by monthly/bimonthly computational tomography. Cas9-CR tumor-free and overall survival will be measured in comparison to *Kras*^{G12D} only mice, with *Znfx1* knock-out only mice, and with non-induced mice. Lung tumors profiles will be analyzed by histopathology analyses and molecular analyses (e.g. tumor programs, immune response/inflammation programs). Thus, the establishment of this new mouse model will open new perspectives for the investigations on the impacts of *ZNFX1* in NSCLC tumorigenesis and treatment response.

Definitive radiation therapy for early-stage cancer of the hypopharynx and supraglottis

Travis Hoover, MD,¹ Kai Sun, MS,¹ Jason K. Molitoris, MD, PhD,¹ and Matthew J. Ferris, MD¹

¹Department of Radiation Oncology, University of Maryland School of Medicine, Baltimore, MD

Purpose:

Early-stage cancer of the hypopharynx and supraglottis is managed with either larynx-preserving surgery or definitive radiation therapy (RT). However, early presentations in these head and neck sites are clinically rare, and optimal radiation-based approaches remain sparsely described. We sought to determine whether intensification beyond daily fractionated radiation alone is warranted.

Methods:

We reviewed records of all patients with T1-2N0 squamous cell carcinoma involving the hypopharynx or supraglottis (including glottic tumors with supraglottic extension) treated with definitive RT at our institution between 2010-2024. Patients were excluded if they received prior head and neck RT. Locoregional control and survival were analyzed using chi-squared and Kaplan-Meier tests, respectively.

Results:

With a median follow-up of 25 months (interquartile range 14-54 mos), 48 patients were included. The primary site of disease was supraglottis in 25/48 (52.1%; 15 epiglottis, 4 aryepiglottic fold, 4 false cord, 2 arytenoid), glottis with supraglottic extension in 17/48 (35.4%), and hypopharynx in 6/48 (12.5%; 5 piriform sinus, 1 posterior pharyngeal wall). Most patients (90%) had a smoking history. Histologic diagnoses included squamous cell carcinoma (47/48) and large-cell neuroendocrine carcinoma (1/48). Most patients with supraglottic and hypopharyngeal primaries were treated with volumetric-modulated arc therapy (VMAT) (26/31) or proton therapy (3/31) with bilateral elective lymph node coverage, while either VMAT (9/17) or 3-dimensional conformal RT (8/17) was used for glottic primaries. Thirty patients (62.5%) were treated to 66-70 Gy with conventional fractionation (convF) (23) or accelerated fractionation (accF, 6 fractions per week) (7), 12 patients (all were primary glottic cancers) to 63-65.25 Gy with hypofractionation (hypoF, 2.25 Gy per fraction), and 3 patients to 74.4 Gy with twice-daily hyperfractionation (hyperF). Six patients received concurrent cisplatin. There were 7 recurrences in total (14.6%), of which 6 were local and 1 was in the contralateral neck. All recurrences occurred in patients treated with convF or hypoF RT alone, while no recurrence occurred following accF or hyperF RT or concurrent chemo-RT (cCRT) (7/33 vs. 0/15, $p=0.054$). Among patients with supraglottic or hypopharyngeal primaries, all 3 recurrences occurred following convF RT alone, versus none following accF or BID RT or cCRT (3/18 vs. 0/13, $p=0.121$). Grade 4-5 long-term toxicity occurred in 3 patients (6.3%). Larynx preservation rate was 79%. Two-year overall survival, recurrence-free survival, and laryngectomy-free survival were 78%, 70%, and 68%, respectively.

Conclusion:

An exclusively locoregional recurrence pattern and absence of failures with treatment intensification via accF, hyperF, or cCRT suggests these strategies may be preferable to convF or hypoF for early-stage cancers involving the supraglottis or hypopharynx.

Graph-Based Radiomics: Enhancing Stability and Reproducibility in AI-Driven Multi-Institutional Head and Neck Cancer Analysis

Abstract

Purpose

Radiomics extracts imaging biomarkers but feature variability across institutions and parameter settings limits clinical utility. This study proposes Graph-Based Feature Selection (Graph-FS) to improve feature stability and cross-institutional reproducibility in head and neck squamous cell carcinoma (HNSCC).

Materials and Methods

Graph-FS constructs feature graphs to identify clusters of correlated radiomic features, selecting the most representative ones without labels. From the Gross Tumor Volumes (GTV) of 752 HNSCC patients across three institutions, 1,648 radiomic features were extracted.

Feature stability was evaluated across 36 radiomics parameter settings (including normalization scales, bin widths, and outlier thresholds) using the Jaccard Index (JI), Dice Similarity Coefficient (DSC), and Overlap Percentage (OP). Reproducibility across institutions was assessed using JI, with consistency further evaluated using Kendall's W. Graph-FS performance was compared against conventional methods, including Lasso, Boruta, Recursive Feature Elimination (RFE), and Minimum Redundancy Maximum Relevance (mRMR). Additionally, the model's performance in 2-year survival prediction was assessed using five classifiers.

Results

Graph-FS outperformed conventional methods in terms of stability across parameter settings, with $JI = 0.46$, $DSC = 0.62$, and $OP = 45.8\%$. These results were significantly higher than those for Boruta ($JI = 0.005$), Lasso ($JI = 0.010$), RFE ($JI = 0.006$), and mRMR ($JI = 0.014$). In terms of cross-center reproducibility, Graph-FS achieved the highest JI (0.127) compared to Boruta (0.005), Lasso (0.010), RFE (0.006), and mRMR (0.014). For 2-year survival prediction, Graph-FS achieved the highest AUC (0.71), outperforming Boruta (0.62), Lasso (0.48), RFE (0.50), and mRMR (0.55).

Conclusions

Graph-FS improves feature stability across parameter variations and enhances reproducibility across institutions, outperforming widely used feature selection methods. Our findings reveal that traditional rank-based selection methods are prone to variability across parameter settings, leading to inconsistent feature rankings. This advancement strengthens biomarker reliability and supports the broader clinical integration of radiomics-driven decision-making in precision oncology.

Keywords: Radiomics, Quantitative Imaging Biomarkers, Graph-Based Feature selection Methods, Reproducibility

Innovation/Impact: The reproducibility of scientific findings is not just a cornerstone of research but a critical barrier to clinical translation, particularly in radiomics. Variability in datasets, methodologies, and parameter settings often undermines the reliability of selected features. Traditional feature selection methods, including filter methods (e.g., mRMR), wrapper methods (e.g., Boruta), and embedded techniques (e.g., Lasso), aim to reduce dimensionality and improve model performance. However, these methods often struggle with reproducibility due to their sensitivity to variations in cross-validation splits, model parameters, and dataset composition. Our study addresses this challenge by developing a novel Graph-Based Feature Selection (Graph-FS) method to identify stable and reproducible features.

Methods and results: The workflow of Graph-FS is illustrated in Figure 1, which outlines the feature graph construction and selection process. Figure 2 presents stability across radiomics parameters for each center. Figure 3 compares the reproducibility of various feature selection methods. These results demonstrate the superior performance of Graph-FS in maintaining consistent feature sets across datasets and parameter settings.

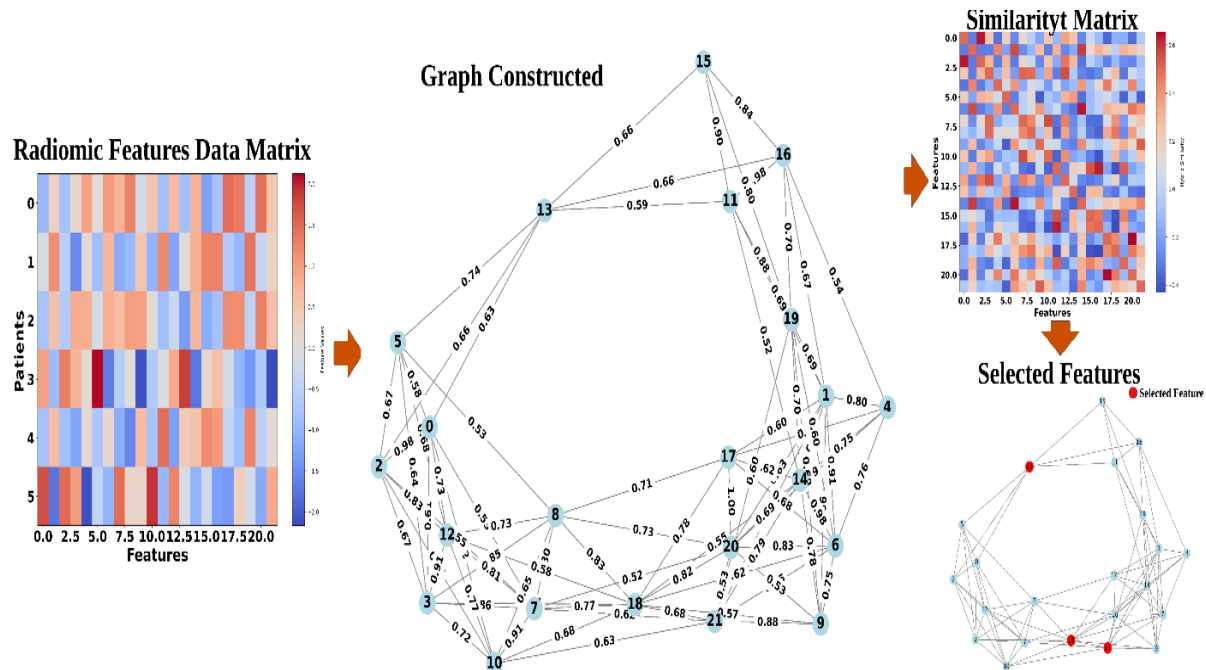


Figure 1. Workflow of Graph-Based Unsupervised Feature Selection (GB-UFS) in Radiomics.

This figure illustrates the general workflow of GB-UFS applied to a sample radiomics feature data matrix with six patients (rows) and 22 features (columns). The radiomics feature matrix is normalized to reflect feature values across patients. A graph is constructed using a similarity matrix, which can be generated through various methods, such as pairwise Spearman correlation, cosine similarity, modular information, or Laplacian computation. Nodes represent features, and edges indicate their similarity. The resulting similarity matrix is used to identify clusters of related features, with the most representative features highlighted as red nodes.

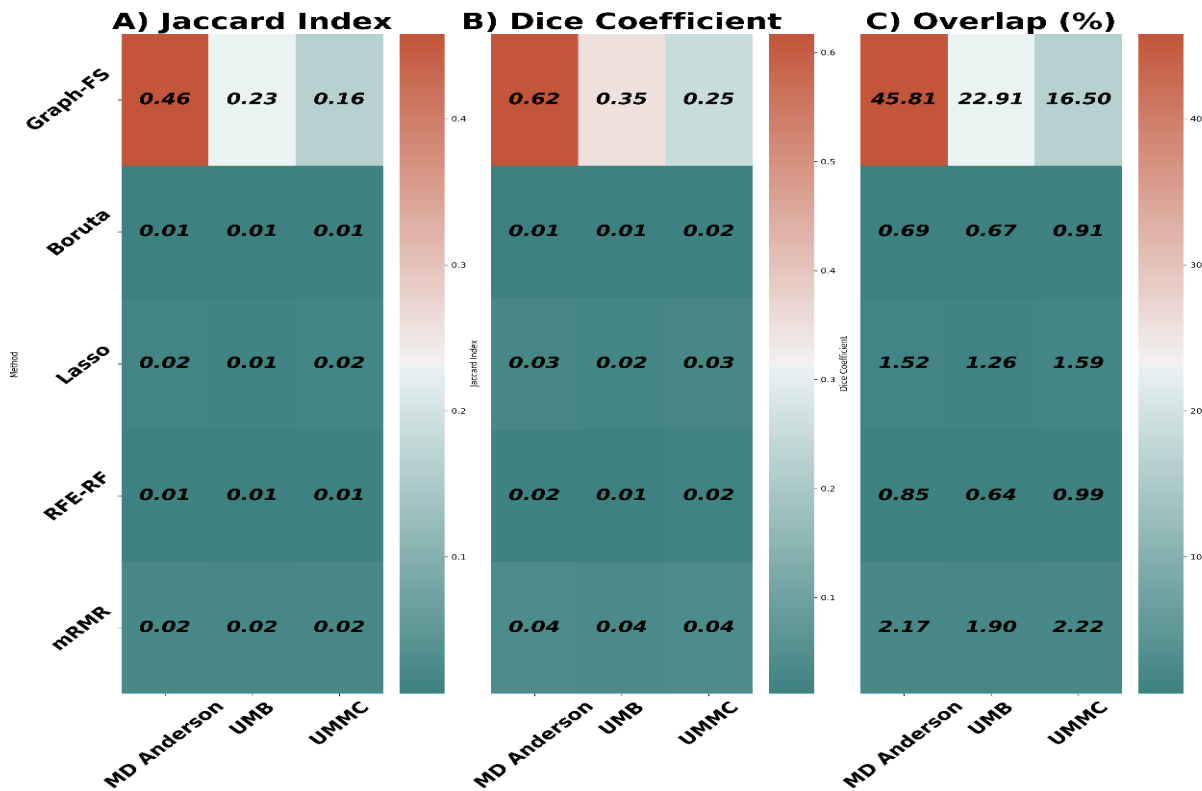


Figure 2. Heatmap of Stability of Feature Selection Methods Across different Radiomics setting parameters within each center: University of Maryland, Baltimore (UMB), University of Texas MD Anderson Cancer Center (MD Anderson), and University MAASTRO Medical Center (UMMC). A) Dice Coefficient is a measure of overlap between feature sets, B) Jaccard Index is a measure of similarity between selected feature sets, and C) Overlap (%) is the percentage of shared features between centers.

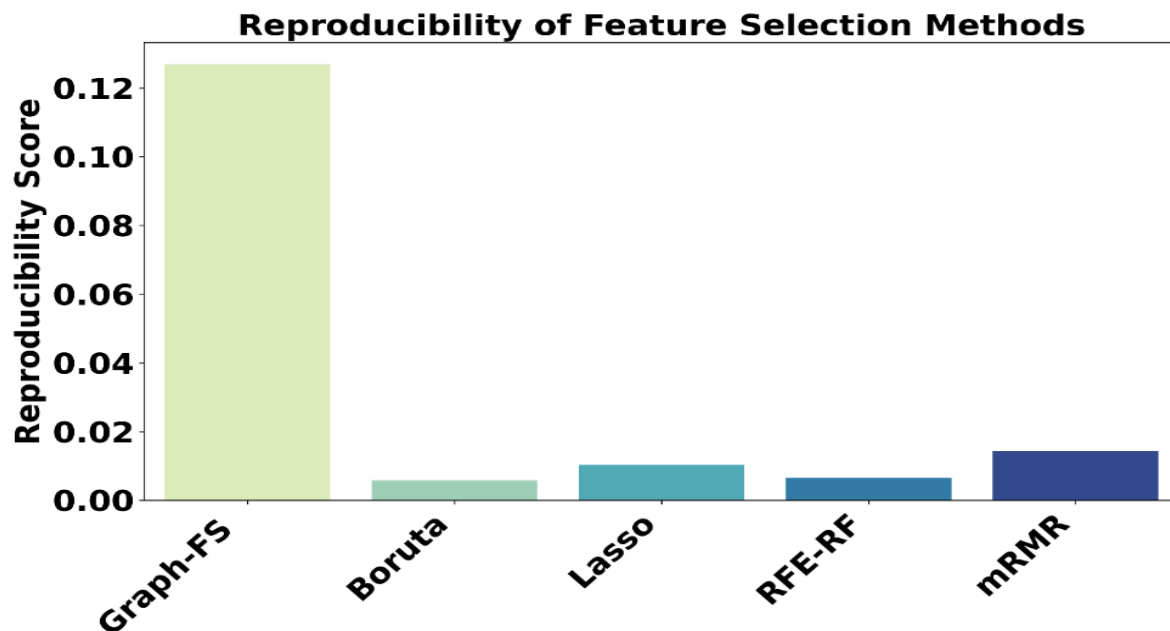


Figure 3. Bar Plot of Feature Selection Reproducibility Scores Across Multiple Centers. This bar plot illustrates the reproducibility scores of various feature selection methods across different medical centers. Higher scores reflect more consistent feature selection across centers, indicating higher reproducibility.

Clinical validation of the role of Caveolin-1 in radiation and chemotherapy resistance in lung cancer

Sanjit Roy¹, Binny Bhandary¹, Zach Keepers¹, Alexander Mackerell², France Carrier¹, Terrence Williams³, Hem D Shukla¹

¹Department of Radiation Oncology, University of Maryland School of Medicine, Baltimore, MD.

²Department of Pharmaceutical Sciences, University of Maryland School of Pharmacy.
Baltimore, MD

³Department of Radiation Oncology, City of Hope, Duarte, CA.

Non-small cell lung cancer (NSCLC) remains one of the most aggressive malignancies and makes up about 85% of all lung cancer cases. For NSCLC patients, where resection surgery may not be feasible, chemoradiation therapy (CRT) and immunotherapy constitute the standard of care treatment. Despite treatment with CRT, NSCLC often recurs and displays resistance to CRT. In this setting, relapsed NSCLC cases are frequently re-irradiated with poor outcomes such as tumor aggression and resistance. Consequently, it is one of the foremost challenges to develop effective therapeutic options to overcome CRT resistance in lung cancer. We have identified upregulation of Caveolin-1 (CAV1) in radiation resistant A549 lung cancer cells and its role in CRT resistance, and tumor aggression. CAV1 is a 21 kDa membrane protein enriched in caveolae and functionally associated with endocytosis, cell migration, metastasis, and CRT resistance. We also observed that knocking out of CAV1 by CRISPR-Cas9 in radioresistant cells reverted to radiosensitive phenotypes. We also created orthotopic lung cancer in athymic nude BALB/c nude mice using A549 parental and radioresistant cells and tumor growth was monitored by CBCT scan using SARRP platform. Animals were treated with 4 and 6 Gy of RT and at study endpoint tumor tissues were analyzed for CAV1 expression. The data showed an elevated level of CAV1 expression in radioresistant resistant tumor. We also performed CAV1 staining and quantification of CAV1 in 55 lung cancer tissue samples and the data showed high expression level of caveolin-1 in stage II and III lung cancer tissues. The TCGA data analysis of 200 lung cancer samples showed genomic alteration of CAV1 in 25 lung cancer samples which was linked to the worst prognosis in lung cancer patients. The upregulation of CAV-1 has also been reported in clinical samples following tumor relapses after treatment with EGFR-osimertinib inhibitor underscoring role of CAV1 in therapy resistance. Currently, we are screening a virtual library of small molecules using Caveolin-1 Cryo-EM structure (PDB ID: 7SCO) to identify potential leads to inhibiting Caveolin-1 functional activity by examining their effect on radio and chemosensitivity in lung cancer cells and animal models of lung cancer.

investigate the role of Caveolin-1 in chemotherapy and RT resistance and develop specific caveolin-1 inhibitors to reverse CRT resistance in lung cancer patients. **Based on our current investigations and published research, Caveolin-1, a 21 kDa membrane protein which is several folds upregulated in A549 radiation and chemoresistant A549 lung cancer cells and plays a role in CRT resistance and cell proliferation.** The TCGA data analysis has also demonstrated Caveolin-1 genomic alterations which is linked with worst prognosis in lung cancer patients. In the proposed grant we will examine Caveolin-1 expression pattern in different stages of lung cancer tissues and correlate its expression with stages of lung cancer and its clinical outcome. Importantly, we will also investigate Caveolin-1 interaction with EGFR, TGFβ, CAV2, FYN kinase and SRC kinase and their concerted role in CRT resistance and tumor aggression. We will generate 3 CAV1 gene mutations V7A, E20K and V170A reported in lung cancer patients in A549 and H226 by CRISPR-Cas9 and examine their role in CRT resistance and tumor aggression. Finally, we will screen Caveolin-1 specific small molecule inhibitor library using CADD (computer aided drug design) approach and test promising small molecule inhibitors in A549 and H226 lung cancer cell line and animal model of lung cancer. This will pave the way for chemo and radio sensitize lung tumor to chemotherapy and radiation therapy treatment in clinical settings.

Assessment of a Novel Snout-Mounted Imaging System for Dose Depth Monitoring

Vijay Raj Sharma, Ph.D.¹, Jie Zhang, PhD², Ehsan Shakeri, Student⁴, Ananta Raj Chalise, PhD⁵, Sina Mossahebi, PhD², Stephen W. Peterson, PhD⁶, Matthias K Gobbert, PhD⁷, Lei Ren, PhD³ and Jeremy C. Polf, PhD⁸

Affiliations

(1)University of Maryland, School of Medicine, Baltimore, MD,

(2)University of Maryland School of Medicine, Baltimore, MD,

(3)University of Maryland, Baltimore, MD,

(4)University of Maryland Baltimore County, Baltimore, MD,

(5)Cleveland Clinic, Cleveland, OH,

(6)Department of Physics, University of Cape Town, Rondebosch, Cape Town, South Africa,

(7)University of Maryland, Baltimore County, Baltimore,

(8)M3D, Inc, Ann Arbor, MI

Purpose: We are developing a novel Compton Camera (CC) system mounted orthogonally on the treatment nozzle for prompt gamma (PG) imaging-based proton range verification during treatment. This study investigates the efficacy of the imaging system and methods to improve the image quality.

Methods: Monoenergetic point sources (ranging: 511 keV to 5 MeV) were positioned within a patient phantom and water models using the Geant4-toolkit to assess depth-dependent gamma-counts. The CC was mounted on the treatment nozzle in a fixed configuration. Data-acquisition focused on recording double-and-triple event interactions, where gamma photons underwent one or two Compton scatters followed by absorption, respectively. These specific interactions were selected to reconstruct gamma emission hotspots accurately while avoiding noise from higher-order interactions. A kernel-weighted back-projection (KWBP) method with fixed parameters was employed to process the recorded data. Proton simulations were conducted at three distinct clinical energies within the same experimental setup, generating a comprehensive dataset of PG emissions from inelastic interactions. An iterative convolution post-processing method was introduced to correct distorted gamma images, significantly enhancing the clarity, ranges, and shape of the experimental reconstructed PG data. This method involved iterative convolution operations using point source data to refine the proton-simulated gamma images.

Results: Lower-energy gamma sources showed higher counts near the phantom surface, with an exponential attenuation behavior observed with depth. Reconstructed images demonstrated the robustness of KWBP algorithm for gamma imaging with known point sources. However, when applied to prompt gamma event data from proton simulations, the KWBP algorithm struggled to accurately reconstruct the images, resulting in shallower images. The introduction of the convolution-based post-processing point source correction method significantly improved range accuracy, shifting gamma spots from 115 mm to 33 mm from proton max-range.

Conclusion: The simulation results strongly support the new experimental-design for the Snout-Mounted-CC System, provided that image corrections are applied.

Investigating Genetic Mechanisms of Tumorigenesis in Non-Small Cell Lung Cancer Transgenic Mice using Tumor Barcoding with Barcode Deep-Sequencing

Authors:

Danielle N. C. Waters^{1*}, Dipanwita Dutta Chowdhury¹, Jinhee Chang¹, Athar Khalil³, Zachary Faber⁴, Alexander Crane³, Triet Nguyen^{1,2}, Shreya Jagtap⁵, Aaron Chan¹, Muhammad Ajmal Khan¹, Audrey Lafargue¹, Christopher McFarland³, Phuoc T. Tran¹.

Affiliations:

¹Department of Radiation Oncology, Division of Translational Radiation Sciences, University of Maryland Baltimore, School of Medicine, Baltimore, MD, USA.

²Department of Biochemistry and Molecular Biology, Johns Hopkins University, School of Public Health, Baltimore, MD, USA.

³Department of Genetics and Genome Sciences, Biomedical Research Building, Case Western Reserve University, School of Medicine, Cleveland, OH, USA.

⁴Mouse Behavioral Phenotyping Core, Cystic Fibrosis Research Center, Case Western Reserve University, School of Medicine, Cleveland, OH, USA.

⁵ Department of Cellular and Molecular Medicine, Johns Hopkins University, School of Medicine, Baltimore, MD, USA.

* Presenter

Abstract

Non-small cell lung cancer (NSCLC) is the most common type of lung cancer, accounting for 85% of lung cancer cases. *KRAS* mutant lung cancers comprise 25-30% of NSCLC cases and have been labeled “undruggable” target due to the biochemical structure of the KRAS protein. It has also been shown that TWIST1 is an essential transcription factor during development and has been implicated in cancer given its role as a key mediator of epithelial-mesenchymal transition (EMT), and its ability to inhibit apoptosis and senescence and induce chemoresistance in *KRAS* mutant NSCLC. Currently, standard care for NSCLC locally advanced patients includes a combination of chemoradiation with adjuvant immunotherapy. NSCLC genetically engineered mouse models (GEMMs) allow unique system to study translational therapeutic studies but one significant drawback of current GEMMs is their limited capacity to generate diverse genotypes and their inadequate quantitative precision. Therefore, we propose that tumor barcoding with barcode deep-sequencing (Tuba-seq) will allow overcoming this limitation by enabling lineage tracing and quantification of chemoradiation treatment impacts on varied genetic backgrounds in the same mouse *in vivo*, offering insight into the radio chemoradiation-pharmacogenetic landscape of NSCLC. To this end, we have generated an inducible lung epithelium specific *Kras*^{G12D}-*Twist1*-*Cas9* NSCLC GEMMs. Next, we will quantify the tumor suppressive and oncogenic effects of multiple candidate genes in NSCLC GEMMs using a combination of Tuba-seq and CRISPR/ Cas9-mediated *in vivo* genome editing.

Treatment plan LET validation using measured integral depth dose for proton therapy

Nrusingh C. Biswal^{1,2}, Ajay Banskota², ByongYong Yi^{1,2}, Weiguang Yao^{1,2}

¹Department of Radiation Oncology, University of Maryland School of Medicine, Baltimore, MD 21201, USA

²Maryland Proton Treatment Center, Baltimore, MD 21201, USA

Main topic	Clinics
Subtopic	LET and variable RBE-based particle therapy

Abstract (346/350 words):

Background and Aims: Biological effects associated with proton therapy, e.g. Linear energy transfer (LET) dependent relative biological effectiveness (RBE) dose in proton therapy have been of recent interest. LET is an important value to be validated especially for the concerned organs at risk (OARs) before treatment. However, it imposes a bottleneck in measuring LET due to very limited techniques available. Here we propose a new efficient method for patient-specific LET validation for the OARs in the proton treatment planning.

Methods: The beam-specific depth of the concerned OAR in the patient was converted to a depth in a solid water phantom by matching the shapes of TPS calculated LET distributions in the patient CT and phantom. The IDD at the determined depth in the phantom was acquired by a multilayer ionization chamber (IC). A collimator made up of 2 cm thick copper with a 1 cm diameter opening was placed in front of the IC to collect those protons of interest. The beam contributing the largest LET onto the OAR in the plan was delivered to the phantom. The energy spectrum of the protons was extracted from the IDD, and the LET was calculated from the energy spectrum (Figure 1). A comparison of the measured and the TPS calculated dose-averaged LET (LET_d) on the brainstem was done for 7 brain and 1 head-and-neck (HN) tumor patients. For all 8 patients, a total of 30 measurements were done in the ROIs within 7-15 cm depths.

Results: For all the 30 measurements, the LET_d ranged between 2.9 to 13.1 keV/ μ m, while the corresponding LET_d from the TPS ranged from 2.5 to 13.7 keV/ μ m. The differences between measurement and TPS were within -1 to +0.6 keV/ μ m. In 23 of 30 cases, the LET_d was higher for the measurement than that of the TPS. There was a strong correlation between the calculated and measured LET_d with R^2 of 0.974 (Figure 2).

Conclusions: Our proposed method was used to successfully validate the treatment planning system calculated dose-averaged LET (LET_d). This may be a potential tool to QA the LET doses on the organs at risks during proton therapy.

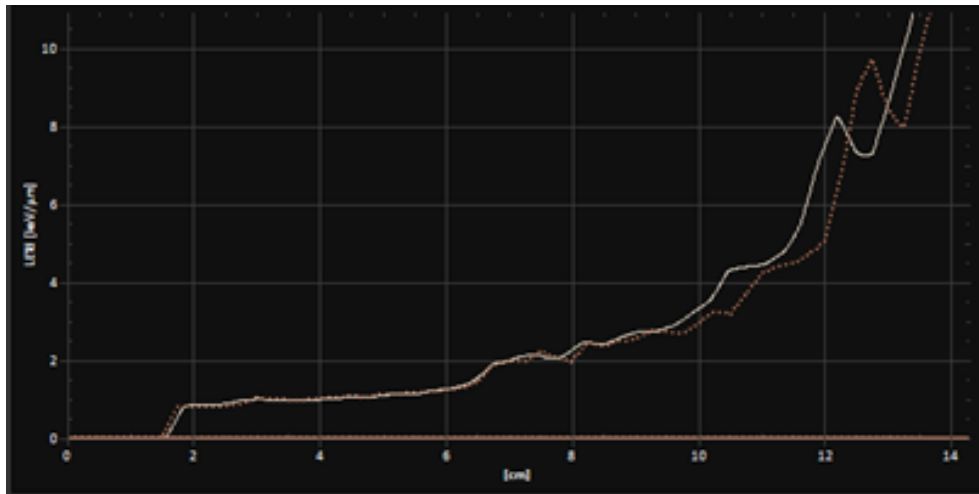


Figure 1: displays how to determine the depth in solid water phantom for an OAR in the patient. Solid curve: LETd along the beam path in the treatment plan. Dotted curve: LETd along the beam path in the solid water phantom. The curves are matched at a depth < 7 cm because the muscle in this region has a similar density to that of the phantom. The curves are not matched at depth > 7 cm because the beam passes through bony structures, but the shapes of the curves are like each other. If the OAR is at depth 10 cm, then from the shapes, we determine the depth in the phantom as 10.5 cm.

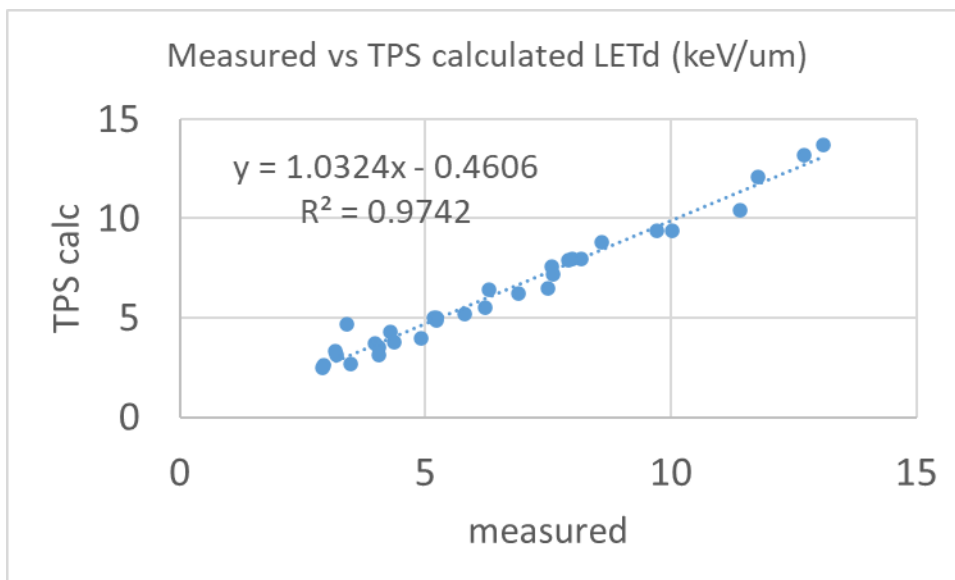


Figure 2: LETd measured vs TPS calculated.

Twist1* Overexpression Models an Aggressive Subtype of Pancreatic Ductal Adenocarcinoma *in vivo

Muhammad Ajmal Khan^{1, *}, Jinhee Chang^{1,2, *}, Yang Song¹, Amol C. Shetty¹, Triet Nguyen^{1,2}, Danielle N. Waters¹, Dipanwita Dutta Chowdhury¹, Elan Simms¹, Aaron Chan¹, Christine Lam², Priyanshi Patel¹, Lucas T. Tran¹, Jiayu Chen², Jarey H. Wang², Katriana Nugent², Matthew Ballew², Ghali Lemtiri-Chlieh², Francesca Anna Carrieri^{1,2}, Reem Malek², Hailun Wang^{2,3}, Noelle R. (Jurcak) Thielman⁴, Keyu Li⁵, William L. Hwang⁶, Lei Zheng⁷, Kathleen Gabrielson⁸, Phuoc T. Tran^{1,2,7,9,#}, Audrey Lafargue^{1,2, #}

Affiliations:

¹Department of Radiation Oncology, Division of Translational Radiation Sciences, University of Maryland Baltimore, School of Medicine, Baltimore, MD, USA.

²Department of Radiation Oncology and Molecular Radiation Sciences, Johns Hopkins University, School of Medicine, Baltimore, MD, USA.

³GenoImmune Therapeutics, Wuhan, China.

⁴Department of Immunology and Microbiology, Lake Erie College of Osteopathic Medicine, Erie, PA, USA.

⁵Department of Pancreatic Surgery West China Hospital, SCU Chengdu 610041, P. R. China.

⁶Center for Systems Biology, Center for Cancer Research, Department of Radiation Oncology, Massachusetts General Hospital and Harvard Medical School, Boston, MA, USA.

⁷Department of Oncology, Sidney Kimmel Comprehensive Cancer Center, Johns Hopkins University, School of Medicine, Baltimore, MD, USA.

⁸Department of Molecular and Comparative Pathobiology, Johns Hopkins University, School of Medicine, Baltimore, MD, USA.

⁹Department of Urology, James Buchanan Urological Institute, Johns Hopkins University, School of Medicine, Baltimore, MD, USA.

***Equal contribution**

#Corresponding authors: Phuoc T. Tran, MD, PhD - phuoc.tran@umm.edu. Audrey Lafargue, PhD - alafargue@som.umaryland.edu. Address: University of Maryland Baltimore, School of Medicine, 655 West Baltimore Street, Bressler Research Building, Rm 8-020, Baltimore, MD 21201, United States of America. *Phone:* +1 (410) 706 1339.

ABSTRACT

Pancreatic ductal adenocarcinoma (PDAC) is a lethal cancer with distinct molecular subtypes. The Quasimesenchymal/Squamous/Basal-like (QSB) subtype has the worse prognosis with upregulation of epithelial-mesenchymal transition (EMT) transcription factor *TWIST1*. However, no *in vivo* models exist for QSB subtypes. We hypothesized that *TWIST1*-dependent plasticity program drives QSB PDAC subtype development. We performed non-negative matrix factorization (NMF) for human PDAC subtypes using TCGA dataset. We generated a novel tetracycline-inducible autochthonous pancreas specific *Kras*^{G12D}-*Twist1* (PGRT) cancer genetically engineered mouse model (GEMM). *Twist1* and *Luciferase* expression in pancreatic epithelium of PGRT mice was activated through doxycycline (DOX) administration. Our human

NMF analysis identified 3 clusters with NMF1 dominated by QSB subtype, highest *Twist1* expression and worst overall survival (OS). PGRT model showed accelerated tumor development and reduced OS compared to PGR (*Kras*^{G12D} alone) mice (4.6 months vs 9.7 months, $P < 0.0001$). Our histological and IHC analyses showed that PGRT pancreatic tumors spanned a spectrum of PDAC to QSB subtype correlating with length of time of *Twist1*-dependent induction. Vimentin overexpression and squamous histology correlated with *Twist1*-driven EMT in PGRT tumors. Furthermore, PGRT mice had increased metastases (9.52 % PGR at 48 Weeks vs 73.91% PGRT at 24 weeks, $p < 0.0001$). PGRT tumors demonstrated transcriptomic profile linked to collagen content, EMT, cell movement and aligned with human QSB and squamoid single-cell PDAC molecular subtype. Altogether, *Twist1* overexpression with *Kras*^{G12D} drives PDAC development and metastasis, mimicking human QSB PDAC subtypes. This novel model could offer new perspectives on PDAC and enables testing therapeutics to improve QSB PDAC patient outcomes.

Key Words: pancreatic ductal adenocarcinoma, *Twist1*, epithelial-mesenchymal transition

Enhancing Image Quality in Acoustic Imaging Using the Segment Anything Model (SAM)

Yankun Lang, Zhuoran Jiang, Leshan Sun, Liangzhong Xiang, Lei Ren

Purpose/Objectives: Electroacoustic tomography (EAT) and Protoacoustic (PA) imaging are novel modalities for treatment verification of electroporation and proton therapy. However, the limited acquisition angle in both EAT and PA imaging induces severe image distortion, limiting their verification accuracy. This study aims to develop SAM-Med3D, a 3D segmentation large model, to enhance PA and EAT images to correct image distortion to achieve precision treatment verification.

Method/Materials: The SAM-Med3D model was enhanced by modifying its encoder-decoder architecture. A global-local feature fusion strategy in the encoder preserved structural details, while a lightweight decoder incrementally improved image resolution. The model was trained to refine distorted acoustic images to match ground truth. The EAT dataset consisted of 30 scans of water and tissue phantom (chicken and pork) using various electrode settings (2 electrodes, various distances, and angles) and voltages (600–1000 Volts/cm). 120 views equally distributed over 360° were acquired using a matrix array in each scan. The PA imaging dataset consisted of 126 prostate proton therapy patients . The protoacoustic signals were simulated based on CT and planned dose for an ultrasound matrix array (64×64 size, 500kHz central frequency) placed under the perineum. Data splittings for EAT and PA images are 1:1 and 3:1, respectively.

Results: Image enhancement was evaluated on 15 EAT and 40 prostate PA images. Metrics included PSNR/SSIM (38.24/0.98 for EAT) and RMSE/SSIM (36.01/0.95 for PA). The enhanced pressure map demonstrated high accuracy, with a total processing time of ~ 1 s.

Conclusion: The application of SAM-Med3D in PA and EAT imaging offers a viable solution to the limited-angle problem, facilitating high-precision 3D dose verification in proton therapy. This study underscores the potential of large-scale models like SAM-Med3D for advancing image enhancement techniques in medical imaging, particularly in the context of real-time radiation therapy monitoring.

DNMTi in combination with PARPi inhibits aberrant WNT/Beta-catenin and Tenascin C pathway signaling, decreasing cancer stemness and metastasis in triple-negative breast cancer

Kaushlendra Tripathi^{1,2}, Lora Stojanovic^{1,2}, Michael J. Topper⁴, Stephen B. Baylin^{4, 5*}, Kenneth P. Nephew^{3,6,24*}, Feyruz V. Rassool^{1,2*}

¹University of Maryland Marlene and Stewart Greenebaum Comprehensive Cancer Center, Baltimore, MD 21201, USA. ²Division of Translational Radiation Sciences, Department of Radiation Oncology, University of Maryland School of Medicine, Baltimore, MD 21201, USA. ³Medical Sciences Program, Indiana University School of Medicine-Bloomington, Bloomington, IN 47405, USA. ⁴Department of Oncology, The Sidney Kimmel Comprehensive Cancer Center at Johns Hopkins, Baltimore, MD 21231, USA. ⁵Van Andel Research Institute, Grand Rapids, MI 49503, USA. ⁶Department of Anatomy, Cell Biology and Physiology, Indiana University School of Medicine Indianapolis, ⁷Indiana University Melvin and Bren Simon Comprehensive Cancer Center, Indianapolis, IN 46202, USA.

Triple-negative breast cancer (TNBC) has a higher rate of metastasis, a poorer prognosis and survival compared with other breast cancer types. Poly-ADP ribose polymerase inhibitors (PARPis) are used to treat TNBC patients that harbor germline BRCA1/2 mutations, inducing synthetic lethality, but responses are not durable. We previously reported that PARPis, in combination with DNA methyltransferase inhibitors (DNMTis), exert synergistic cytotoxicity in TNBC, independent of BRCA mutations, but the effects of this drug combination on metastasis and stemness that are associated with poor survival outcomes are not known. Aberrant Wnt/ β -catenin signaling in TNBC is known to drive cancer stemness, metastasis, and resistance to apoptosis and chemotherapy. To determine the effects of DNMTis and PARPis on these pathways, mouse *in vivo*, metastasis mouse models show that this drug combination decreases metastases to the lung. To elucidate the molecular pathways underlying this drug treatment, we performed RNA seq analysis on MDAMB231 TNBC cells following treatment of DNMTis and PARPis alone and in combination. Hallmark pathway analysis showed that Wnt/ β -catenin signaling cancer stemness, cell migration and metastatic growth are decreased with the drug combination more than single agent treatments. Indeed, analysis revealed decreased expression of leading-edge genes, including down-regulation of tenascin-C (TNC), a multinodular glycoprotein known to promote the migration of cancer cells within the tumor microenvironment, and validated by PCR. To functionally confirm the effects of this drug combination on stemness, we next performed flow cytometry and PCR for stem cell markers pre- and post- drug treatment in TNBC cell lines and patient organoids and showed that there is a decrease in spheroid formation with combination treatment comparison to mock-treated organoids. For cell migration, we performed scratch assays and xCELLigence Real-Time Cell Analysis (RTCA) in MDA MB231 and SUM 159 cells and observed that combination treatment decreased cell migration. Notably, *in vivo*, tail vein injections of MDA MB231 showed decreased metastasis in mice with the combination treatment of AZA and TAL compared to mock-treated cells. To mechanistically elucidate the role of Beta-catenin/TCF12 in regulating downstream targets, we identified Beta-catenin/TCF12 binding sites in the TNC promoter and performed the chromatin immunoprecipitation (ChIP) assay and, for the first time, showed that Beta-catenin/TCF12 binds to the promoter region of TNC. This clearly demonstrates that beta-catenin transcriptionally regulates the expression of TNC by binding to its promoter region. Finally, to mimic the effects of the drug combination, inhibition or KD of Wnt/Beta-catenin or TNC expression decreases the cell migration and stemness in TNBC. Taken together, our results show for the first time that PARPi and DNMTi combination therapy target key pathways, highlighting the key role of WNT/Beta-catenin regulation of TNC in driving aggressive disease and poor survival in TNBC

Keywords

TNBC, DNMT and PARP inhibitors, Wnt/ β -catenin, TNC, stemness, cell migration and metastasis.

3-Bromopyruvate in combination with radiation inhibits pancreatic tumor growth by stalling glycolysis, and dismantling mitochondria in a syngeneic mouse model

Hem D Shukla, Sanjit Roy, Bolutife Olagunju, Binny Bhandary, Zachery Keepers and Ryan William

Division of Translational Radiation, Department of Radiation Oncology, University of Maryland School of Medicine, Baltimore, MD

Pancreatic cancer (PC) is the fourth-most-deadly cancer in the United States with a 5-year survival rate of only 11%. The majority of patients with locally advanced pancreatic cancer undergo chemotherapy combined with radiation therapy (RT). Nevertheless, current treatments are inadequate, and novel strategies are desperately required. 3-Bromopyruvate (3-BP) is a promising anticancer drug against pancreatic cancer. It exerts potent anticancer effects by inhibiting hexokinase II enzyme (HK2) of the glycolytic pathway in cancer cells. The colonogenic survival data showed 80% cell death of Panc-2 cells at 15 μ M concentration, and 95% cell death when treated with 10 μ M of 3-BP and 4 Gy of radiation. 3-BP severely inhibited ATP production by disrupting the interaction between HK2 and mitochondrial Voltage Dependent Anion Channel-1 (VDAC1) protein. The combination of 3-BP and radiation also inhibited β -Catenin pathway, cMyc, TGF- β and MCT1 transporter signaling pathway in Panc-1 and MIA PaCa-2 cells. We further examined therapeutic effect of 3-BP in syngeneic mouse model of pancreatic cancer by treating animals with 10, 15 and 20 mg/kg doses. We observed approximately 65-70% suppression in tumor growth in C57BL/6 animals. Immunohistochemistry data showed complete inhibition of hexokinase II (HK2) and TGF β , in animals treated with 15 and 20 mg/kg of 3-BP drug. We also observed enhanced expression of active caspase-3 in tumor tissues exhibited apoptotic death and mitochondrial damage in treated tumor tissues. Flow Cytometry analysis showed significant inhibition in MDSCs (CD11b) population in treated tumor which may have allowed infiltration of CD8⁺ T cells and inhibited tumor growth. Notably, metabolomic data also revealed severe inhibition in glycolysis, NADP, ATP and lactic acid production in treated cancer cells. These results provide new evidence that 3-BP severely inhibits glucose metabolism in cancer cells by blocking hexokinase II and disrupting mitochondria by suppressing BCL2L1 in pancreatic cancer.

TNFI-induced chemoradiation resistance in small cell lung cancer

Authors:

Dipanwita Dutta Chowdhury^{1,§,+}, Eddie Imada^{2,§}, Nick Connis³, Hwai Wei Tseng¹, Triet Nguyen^{1,4}, Jinhee Chang¹, Danielle Council¹, Aaron Chan¹, Elan Simms¹, Amol C. Shetty⁵, Yang Song⁵, Muhammad Ajmal Khan¹, Audrey Lafargue¹, Mohammad Rezaee⁴, Phuoc T. Tran^{1,4,#}, Luigi Marchionni^{2,#}, Christine L. Hann^{3,#}

Affiliations:

¹Department of Radiation Oncology, Division of Translational Radiation Sciences, University of Maryland Baltimore, School of Medicine, Baltimore, Maryland.

²Department of Pathology and Laboratory Medicine, Weill Cornell Medicine, New York.

³Department of Oncology, Johns Hopkins University School of Medicine, Baltimore, Maryland.

⁴Department of Radiation Oncology and Molecular Radiation Sciences, Johns Hopkins University, School of Medicine, Baltimore, Maryland.

⁵Institute for Genome Sciences, University of Maryland Baltimore, Maryland.

§ Authors contributed equally to this work.

+Presenter.

Corresponding authors: phuoc.tran@umm.edu ; chann1@jhmi.edu ; lum4003@med.cornell.edu

Abstract:

Chemoradiation (CRT) is the standard first-line therapy for limited stage small cell lung cancer (LS-SCLC), which is characterized by early metastasis, intrinsic-acquired CRT resistance and tumor recurrence. CRT confers a 20-25% 5-year overall survival in patients with LS-SCLC. In this study, we utilized patient-derived xenograft (PDX) models to demonstrate CRT resistance of SCLC and identified CRT resistance candidate genes from various SCLC PDX that represent the majority of molecular subtypes (n=4 that include SCLC-A and SCLC-N subtypes). RNA-seq data identified *TNFI* (Traf2- and Nck-interacting kinase) as one such gene that is consistently upregulated in SCLC PDXs exposed to CRT compared to single modality treatments. Copy number gains of *TNFI* were also present in human SCLC samples. Overcoming this CRT resistance is crucial in improving treatment outcomes and patient survival. Genetic depletion or pharmacological inhibition of *TNFI* reduced the *in vitro* clonogenic survival of *TNFI*^{high} SCLC cells, NCI-H446 and makes them increasingly sensitive to CRT. *In vivo*, pharmacological inhibition of *TNFI* with the inhibitor NCB-0846, enhances the CRT sensitivity of NCI-H446 cell line-derived xenografts (CDX) in NOD SCID immunodeficient mice. Furthermore, pharmacological inhibition of *TNFI* *in vivo* demonstrated sensitivity to CRT in LX33 PDX. In conclusion, our results indicate that *TNFI* plays a role in conferring resistance to CRT *in vitro* in SCLC cell lines and *in vivo* in SCLC CDX and PDX models and therefore, can be a potential therapeutic target in limited stage SCLC.

Investigating the Role of TNIK in the Pathogenesis of Lung Squamous Cell Carcinoma

Jinhee Chang¹, Dipanwita Dutta Chowdhury¹, Danielle N. Council¹, Triet Nguyen^{1,2}, Shreya Jagtap¹, Aaron Chan¹, Muhammad Ajmal Khan¹, Nick Connis³, Pedro Torres-Ayuso⁴, John Brognard⁵, Mohammad Rezaee⁶, Audrey Lafargue¹, Christine L. Hann³, Phuoc T. Tran¹.

1. Department of Radiation Oncology, Division of Translational Radiation Sciences, University of Maryland Baltimore, School of Medicine, Baltimore, MD, USA.
2. Department of Biochemistry and Molecular Biology, Johns Hopkins University, School of Public Health, Baltimore, MD, USA.
3. Department of Oncology, Sidney Kimmel Comprehensive Cancer Center, Johns Hopkins University, School of Medicine, Baltimore, MD, USA.
4. Department of Cancer and Cellular Biology, Lewis Katz School of Medicine at Temple University, Philadelphia, Pennsylvania
5. Laboratory of Cell and Developmental Signaling, Center of Cancer Research, National Cancer Institute, Frederick, Maryland
6. Department of Radiation Oncology, Johns Hopkins University, School of Medicine, Baltimore, MD, USA.

Mentor Name: Phuoc T. Tran

Abstract

Lung squamous cell carcinoma (LSCC) is the second most prevalent type of lung cancer with no FDA-approved targeted therapies. Platinum-based chemotherapy and immunotherapy remain the cornerstone of current treatments for advanced LSCC, and the 5-year survival rate is less than 10%. Despite abundant knowledge of the mutational landscape of LSCC, there is a paucity of effective targeted therapies.

Amplification of chromosome 3q26 is the most common genomic alteration in LSCC and this leads to the overexpression of oncogenic kinases like TNIK. TNIK amplification occurs in approximately 50% of LSCC cases and is associated with tumorigenesis and therapy resistance in other cancers. Recent studies showed that TNIK maintains the survival of LSCC cells and drives LSCC progression. Furthermore, inhibiting the kinase eradicates tumor growth in TNIK-high preclinical models. These findings highlight the potential of TNIK as a therapeutic target in a subset of LSCC patients with 3q amplification.

However, one major limitation of previous studies is the lack of animal models with squamous histology and patient-relevant genotypes. Therefore, we have created a novel conditional TNIK-overexpressing genetically engineered mouse model (GEMM) to better understand the roles of TNIK in tumor progression and therapy resistance in LSCC and elucidate mechanisms underlying LSCC pathogenesis.

We are also producing a novel TNIK-overexpressing LSCC GEMM based on the simultaneous activation of KrasG12D and deletion of Fbxw7 (KF model). We will present validation studies such as histological and molecular profiling of our conditional TNIK GEMM and initial data on the TNIK overexpressing LSCC transgenic mouse model (KF (LSCC control) vs KF-TNIK (LSCC-TNIK)).

Noura Radwan, M.D.¹, Matthew P. Deek, M.D.², , Caitlin Eggleston, MPH¹, Kaysee Baker, M.S.¹, Zaker Rana, M.D.¹, Matthew J. Ferris, M.D.¹, Young Kwok, M.D.¹, Sara Dudley, M.D.¹, Soren M. Bentzen, Ph.D., DMSc^{1,3}, Ronald Ennis, M.D.², Lara Hathout, M.D.², Biren Saraiya, M.D.², Tina Mayer, M.D.², M. Minhaj Siddiqui, M.D.⁴, Heather Mannuel, M.D.⁵, Arif Hussain, M.D.⁵, Alejandro Berlin, M.D.⁶, Mark V. Mishra, M.D.¹, Phuoc T. Tran, M.D., Ph.D.¹, Jason K. Molitoris, M.D., Ph.D.¹

1 Department of Radiation Oncology, University of Maryland School of Medicine, Baltimore, MD

2 Department of Radiation Oncology, Rutgers Cancer Institute of New Jersey, New Brunswick, NJ

3 Department of Epidemiology & Public Health, University of Maryland School of Medicine, Baltimore, MD

4 Department of Surgery, University of Maryland School of Medicine, Baltimore, MD, USA

5 Department of Medical Oncology, University of Maryland School of Medicine, Baltimore, MD

6 Department of Radiation Oncology, Princess Margaret Hospital, Toronto, Canada

TRIAL IN PROGRESS

Phase 2 randomized high-risk metachronous oligometastatic prostate cancer with high-risk mutations treated with metastasis directed therapy and niraparib/abiraterone acetate plus prednisone (KNIGHTS) trial

Background: Some patients with oligometastases may have the potential for long-term disease-free survival with just aggressive local therapy as shown by randomized trials for total consolidation of macroscopic metastases using metastasis-directed therapy (MDT). Long-term outcomes of pooled STOMP and ORIOLE trials in oligorecurrent metastatic castration-sensitive prostate cancer (omCSPC) demonstrated MDT improved progression free survival. However, men with high-risk mutations, including pathogenic alterations in *ATM*, *BRCA1/2*, *Rb1*, and *TP53*, did poorly. Additional data suggests men with metastatic castration-resistant prostate cancer and similar mutations are sensitive to PARP inhibition (PARPi) with niraparib. We are launching a first-in-man biomarker-driven trial in omCSPC patients with high-risk mutations to evaluate the efficacy of MDT + androgen deprivation therapy (ADT) *versus* MDT + ADT + niraparib/abiraterone acetate plus prednisone (nira/AAP).

Methods: This study is a multi-site, non-blinded, randomized phase II trial in patients with omCSPC. Men with histologically confirmed (at any site) omCSPC (≤ 3 metastases on standard imaging or ≤ 5 on Axumin/Choline/PSMA-PET/CT) and germ-line/somatic high-risk mutations (*TP53*, *BRCA1/2*, *PALB2*, *ATM*, *BRIP1*, *CHEK2*, *FANCA*, *RAD51B*, *RAD54L*, *MUTYH*) will be randomized (1:1) to MDT + 6- months ADT *versus* MDT + 6-months ADT + 6-months nira/abi. A range of MDT radiation fractionation regimens are permitted. Subjects who meet eligibility criteria and qualify for enrollment will be stratified according to: (i) institution; (ii) conventional/enhanced imaging, (iii) PSADT <6-months, (iv) initial surgery/radiation, and (v) *BRCA1/2* status. This study has been IRB approved (NCT06212583). We assume an accrual time of 24 months, with 18 months of additional follow-up time, and will randomize a total of 88 patients (44 patients in each arm). The primary endpoint will be to assess frequency of PSA failure (> 0.2 ng/mL post primary surgery or nadir + 2 post definitive radiation) with testosterone > 100 ng/dl at 18-months after randomization (powered for 20% improvement over control arm by Fisher's exact test). Secondary endpoints will include toxicity, quality of life (QoL), time to locoregional progression, time to distant progression, time to new metastasis, radiographic progression-free survival, and duration of response. Discovery correlatives associated with clinical outcome will be assessed by collection of including, but not limited to, cell free DNA, circulating-tumor cells, immunologic biomarkers, microbiota and radiomics.

Enhance Four-dimension Cone-beam Computed Tomography (4D-CBCT) From Sparse Views Using A Novel Deep Learning Model

Jie Zhang¹, Lei Ren^{1*}

¹ University of Maryland School of Medicine, Baltimore, USA

Purpose: 4D-CBCT is valuable for imaging anatomy affected by respiratory motions to guide radiotherapy delivery. However, 4D-CBCT often has undersampled projections acquired in each respiratory phase due to the limit in scanning time and dose, severely impacting the image quality. This study aims to enhance its image quality by using a deep learning model to predict full-view projections.

Methods: A deep learning model was developed to use two projections at different angles as the inputs and predict projections at other specified angles. Specifically, the model uses a U-net backbone with our self-designed convolutions to fit the rotation-induced signal variation. The projection at the angle of β (\mathbf{u}_β) is generated according to its two neighbors ($\mathbf{u}_{\alpha1}$ and $\mathbf{u}_{\alpha2}$) in sparse views (SV). $\beta-\alpha1$ and $\beta-\alpha2$ are inputted to our model to generate regulators to modify the model weights, which is to adaptively adjust the contribution ratio of $\mathbf{u}_{\alpha1}$ and $\mathbf{u}_{\alpha2}$. The model was trained and validated using the Elekta 4D-CBCT data from real patients provided by the AAPM SPARE challenge. $\{\mathbf{u}_{\alpha1}, \mathbf{u}_{\alpha2}\}$ and \mathbf{u}_β composed one sample pair. There were 2695 sample pairs from No.1~4 patients for training and 669 pairs from No.5 patient for validation. The generated projections and its reconstructed volumes were compared with the true ones in the challenge data using root mean square error (RMSE), peak signal-to-noise ratio (PSNR) and structural similarity index measure (SSIM).

Results: The predicted projections show comparable quality to the ground truth with a RMSE of 0.154 ± 0.087 , a PSNR of 32.339 ± 4.758 dB and a SSIM of 0.992 ± 0.011 . The volumes are enhanced with a RMSE of 0.002 ± 0.001 (SV: 0.033 ± 0.023), a PSNR of 38.911 ± 3.532 dB (SV: 20.926 ± 10.838) and a SSIM of 0.964 ± 0.019 (SV: 0.407 ± 0.384).

Conclusion: The proposed model predicts full-view projections from a sparse-view 4D-CBCT. It enables high-quality imaging with reduced scan time and dose.

Quantum-inspired genetic optimization tailored for patient scheduling in radiation oncology

Akira SaiToh¹, Arezoo Modiri², Amit Sawant², Robabeh Rahimi²

¹ Department of Computer and Information Sciences, Sojo University, Kumamoto, Japan

² Department of Radiation Oncology, University of Maryland School of Medicine, MD

Purpose: It has been a longstanding challenge to optimize the daily schedule of radiation treatment rooms toward minimum patient wait times, efficient use of clinical staff and reduced running cost of gantries. While genetic algorithms have been one of the most successful workflow optimization algorithms, their complexity becomes a computational burden when solved in classical way. We developed the first of its kind tailored variant of a quantum-inspired genetic algorithm for radiation oncology workflow optimization.

Method: In our design, each quantum-inspired chromosome represented an entire daily schedule consisting of tracks for a single gantry. Each cell possessed two quantum states: (i) a superposition of patient IDs and (ii) a superposition of gantry statuses. The initial generation consisted of 12 randomly generated chromosomes. Simulations were performed on a PC with 16 CPU cores and 32 GB memory. The fitness function was a summation of benefit scores (e.g., completed therapy steps) minus penalty scores (e.g., schedule conflicts). Crossover, mutation, and repair steps were implemented similarly to classical counterparts, with a non-demolition assumption.

Results: For a case study of 3 gantries and 12 patients, the quantum-inspired algorithm achieved the optimization goal in comparable time but with 77% fewer chromosomes than its classical counterpart - 35 versus 150 chromosomes. The surviving, crossover, mutation, and repair ratios were 0.84, 0.27, 0.3 and 0.85, respectively. We showed that the repair ratio has an optimum case-dependent value in the quantum-inspired algorithm in contrast to its continuous positive correlation with fitness growth in the classical algorithm.

Conclusion: We developed a prototype variant of the quantum-inspired genetic algorithm tailored for radiation oncology workflow optimization. The design is extendable to include more variables such as patient room selection. The low quantum memory cost of our algorithm is of practical importance for future (beyond current scope) implementation on quantum computing hardware.

Impact: Genetic algorithms [1,2] are one of the most successful workflow optimization algorithms reported in the literature. The complexity of such algorithms depends on the number of generations, population size, and size of individual chromosomes. This complexity can become a computational burden when solved classically. Here, we propose a prototype quantum-inspired [3-5] genetic algorithm that reduces the required computational resources (# of required chromosomes) while maintaining comparable speed of convergence even with current limited (simulated) quantum processors. Our algorithm has the potential to enhance the efficiency of patient scheduling in radiation oncology [6,7] by minimizing patient wait times and operational costs. Beyond the current scope [8], it can be scaled for scheduling larger departments and to include additional clinically relevant parameters. **Novelty:** We introduce a novel quantum-inspired genetic algorithm for optimizing patient schedules in radiation oncology. Our approach uses quantum superposition principles to represent patient IDs and gantry statuses, resulting in lower computational resource requirements compared to classical counterparts. This is a novel application of quantum-inspired techniques to a practical clinical problem.

Methods: Figure 1 shows the algorithm flow and figure 2 shows the chromosome design. Each chromosome represents a daily schedule for multiple ganties. The color-coded 8 considered

gantry statuses are: idle, ready, waiting for patient, patient positioning, in beam que, beam prepare, beam on, and finally disposing the patient. For the g^{th} gantry and the t^{th} time slot, (g,t) , two quantum states are a superposition of patient IDs, $p(g,t)$ and a superposition of gantry statuses, $s(g,t)$: $|p(g,t)\rangle = \sum_{j=0}^{n_p-1} \alpha_j(g,t)|j\rangle$, $|s(g,t)\rangle = \sum_{k=G_{\text{IDL}}}^{G_{\text{PD}}} \beta_k(g,t)|k\rangle$, $\sum_j |\alpha_j|^2 = 1$ and $\sum_k |\beta_k|^2 = 1$. Initial generation has 12 chromosomes. The Fitness function combines benefit scores (e.g., completed therapy steps) and penalty scores (e.g., schedule conflicts). **Key Results:** Quantum-inspired genetic algorithm is more efficient than the classical one, Fig 3, and it has an optimum repair ratio, Fig. 4.

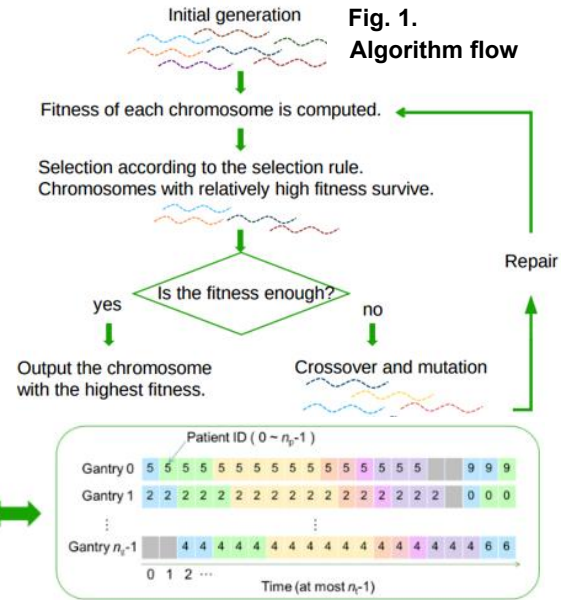


Fig. 2. Chromosome design

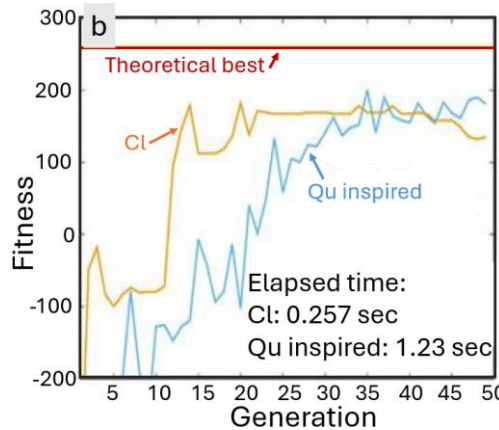
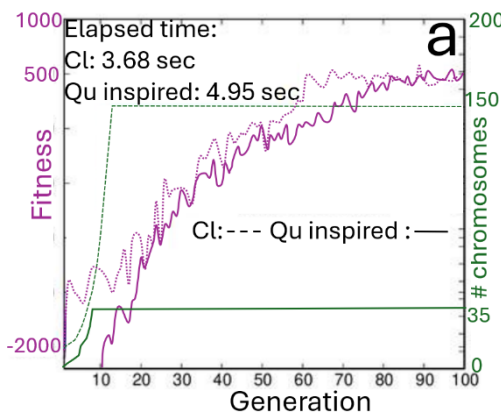
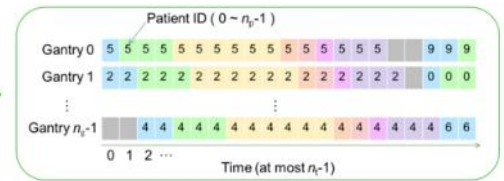


Fig. 3. Classical (Cl) & quantum-inspired (Qu inspired) a) for similar convergence, surviving ratio 0.84, crossover ratio 0.27, mutation ratio 0.3, repair ratio 0.85; b) for where theoretical best is computable, initial #chrom 10, max. #chrom 40 (for both methods), surviving ratio 0.85, crossover ratio 0.4, mutation ratio 0.2, repair ratio 0.87.

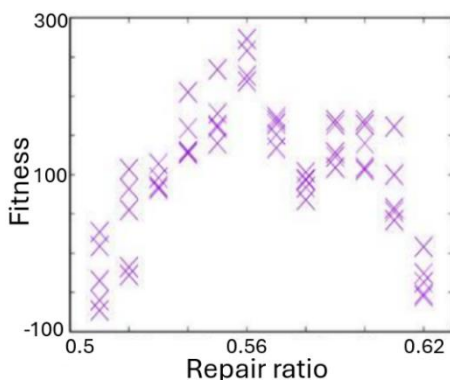


Fig. 4. The repair ratio has an optimum case-dependent value in the quantum-inspired algorithm whereas in classical genetic algorithm the fitness grows with repair ratio.

Acknowledgement: KAKENHI Grant JSPS, Japan (No.18K11344). **References:** [1] Goldberg, Addison Wesley, 1989 [2] Brizuela et al. Proc. GECCO99 (1999) 75-82 [3] Narayanan et al. DOI 10.1109/ICEC.1996.542334 [4] Han et al. DOI 10.1109/TEVC.2002.804320 [5] Nakayama et al. DOI 10.1007/s10015-007-0457-5 [6] Fava et al., DOI 10.1016/j.radonc.2011.11.004 [7] Sakae et al. Jpn. J. Med. Phys. 23(2) (2003) [8] Boixo et al. DOI 10.1038/s41567-018-0124-x.

First Demonstration of Prostate Radiotherapy Plan Optimization on an IBM Quantum Computer

Robabeh Rahimi¹, Akira SaiToh², Arezoo Modiri¹, Yuichiro Nakano³, Ken N. Okada³, Satoyuki Tsukano³, Baoshe Zhang¹, Keisuke Fujii³, Masahiro Kitagawa³, Amit Sawant¹

¹Department of Radiation Oncology, University of Maryland School of Medicine, Baltimore, MD

²Department of Computer and Information Sciences, Sojo University, Kumamoto, Japan

³Center for Quantum Information and Quantum Biology, Osaka University, Japan

Purpose: Fully personalized radiotherapy requires computational resources far exceeding those of conventional CPU/GPU systems. This study explores the use of quantum computing (QC) in radiotherapy planning, both in simulation and on actual quantum hardware, for a simplified, proof-of-concept prostate cancer scenario.

Methods: An objective function used in current treatment planning was converted into binary format, and subsequently to an Ising Hamiltonian for annealing model QC. The Quantum Approximate Optimization Algorithm (QAOA) was applied to the Hamiltonian with a resulting quantum circuit usable for a circuit model QC. In this proof-of-concept study, we considered a bilateral beam plan with one target and one organ at risk (OAR). The target was represented by one volume unit and the OAR by two. For each volume unit, a two-dimensional threshold-dependent high/low level dose was assumed, thus making six qubits sufficient for the implementation. If exact doses were to be considered, qudits (higher dimensional qubits) would be required, which would be out of scope for this proof-of-principle study. The job was submitted to IBM Quantum for simulation and real QC run, and to the D-Wave machine for comparison purposes.

Results: Our quantum circuit was successfully tested using 6 qubits on IBM Quantum both in simulation and on real QC hardware. Validation was performed using the D-Wave machine: For our Ising model Hamiltonian, the optimization returned the ground state, which dosimetrically meant 1.45Gy (assumed prescribed dose) to the target with lower than threshold dose to the OAR confirming the IBM Quantum results.

Conclusion: This study demonstrates the feasibility of using QC for treatment plan optimization in radiotherapy and provides a detailed followable/repeatable framework. The goal beyond current scope is to enable personalized treatment without concerns about computational power limitations.

Impact: Traditional optimization methods in radiotherapy (RT) planning (e.g., gradient descent, simulated annealing) struggle with tackling large databases due to increased computational demands and therefore use approximations. Quantum computing (QC) utilizes superposition and coherence principles to overcome such limitations, enabling comprehensive, personalized treatment planning.

Novelty: While QC in RT optimization has been of great interest [1], to our knowledge, this is the first work that is formulated for and implemented on actual QC hardware. Our work is timely in the emerging field of QC in healthcare. Our QC optimization framework is scalable, with the capacity to formulate and solve larger problems as QC hardware improves. Nazareth et al.'s work, 2015, is the only study of QC in RT optimization that is comparable to ours, however, that work had a high-level presentation & was nonreproducible [2].

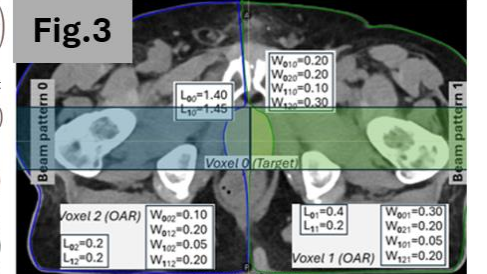
Methods: Figure 1 shows the binary format cost function developed for its conversion to an Ising model Hamiltonian (Fig 2) which is a favorable model for implementation in a quantum annealer system performing quadratic unconstrained binary optimization (QUBO). We defined the dose delivered by the beam pattern k to voxel i as D_{ki} , which included a crude dose, L_{ki} for when the beam directly hit the voxel and a reduced term, W_{kij} , for when another voxel j was in the beam path. The binary variable $x_{ki} = 1$ represented high dose and $x_{ki} = 0$ represented negligibly low dose for the i -th voxel under the k -th beam pattern. We chose to use this high/low two-level dose representation, instead of multilevel dose thresholds, for its simplicity and since a higher dimensional representation would require qudits (instead of qubits), thereby requiring a quantum computer more advanced than the IBM Quantum test platform used in this work. We defined an Ising Hamiltonian representation using the Pauli-Z operator σ_{ki}^z for each voxel i in the beam pattern k and used $\sigma_{ki}^z = x_{ki} - \frac{1}{2}$ to convert our classical binary variable x_{ki} to the quantum mechanical spin representation. Additionally, we introduced a term to eliminate conflicts in processing patterns: e.g., conflict between beam patterns k and l ($k < l$) was formulated as a cost $C_{kl} \in \{0, c\}$ where $c = 0$ & $c \gg 0$ corresponded to non-conflicting & conflicting cases, respectively. No extra qubits were used for Quantum Error Correction. Figure 3 shows the simplified prostate case. This is a hybrid solution where the parameters are calculated within a classical computation (e.g., RayStation treatment planning system for a clinically relevant example) and optimization is performed using QC approaches.

$$\begin{aligned}\tilde{F}_C &= \omega_1 \cdot \tilde{\Delta}_{\text{Target}} + \omega_2 \cdot \tilde{\Delta}_{\text{OAR}} \\ \tilde{\Delta}_{\text{Target}} &= \frac{1}{N_B V_T} \sum_k \sum_{i \in V_T} (-D_{ki} + D_{\text{prescribed, Target}}) \\ \tilde{\Delta}_{\text{OAR}} &= \frac{1}{N_B V_O} \sum_k \sum_{i \in V_O} (D_{ki} - D_{\text{Constraint, OAR}}) \\ D_{ki} &= L_{ki} x_{ki} - \sum_{j \in V_T \cup V_O, j \neq i} W_{kij} x_{ki} x_{kj}\end{aligned}$$

Fig.1

$$\begin{aligned}D_{ki} &= L_{ki} \left(\sigma_{ki}^z + \frac{1}{2} \right) - \sum_{j \in V_T \cup V_O, j \neq i} W_{kij} \left(\sigma_{ki}^z + \frac{1}{2} \right) \left(\sigma_{kj}^z + \frac{1}{2} \right) \\ \hat{H} &= \hat{H}_C + \hat{H}_{\text{Conflict}} \\ &= \frac{1}{N_B V_T} \sum_k \sum_{i \in V_T} (-D_{ki} + D_{\text{prescribed, Target}}) \\ &\quad + \frac{\omega_2}{N_B V_O} \sum_k \sum_{i \in V_O} (D_{ki} - D_{\text{Constraint, OAR}}) \\ &\quad + \sum_{kl (k < l)} C_{kl} \left(\sigma_{k0}^z + \frac{1}{2} \right) \left(\sigma_{l0}^z + \frac{1}{2} \right)\end{aligned}$$

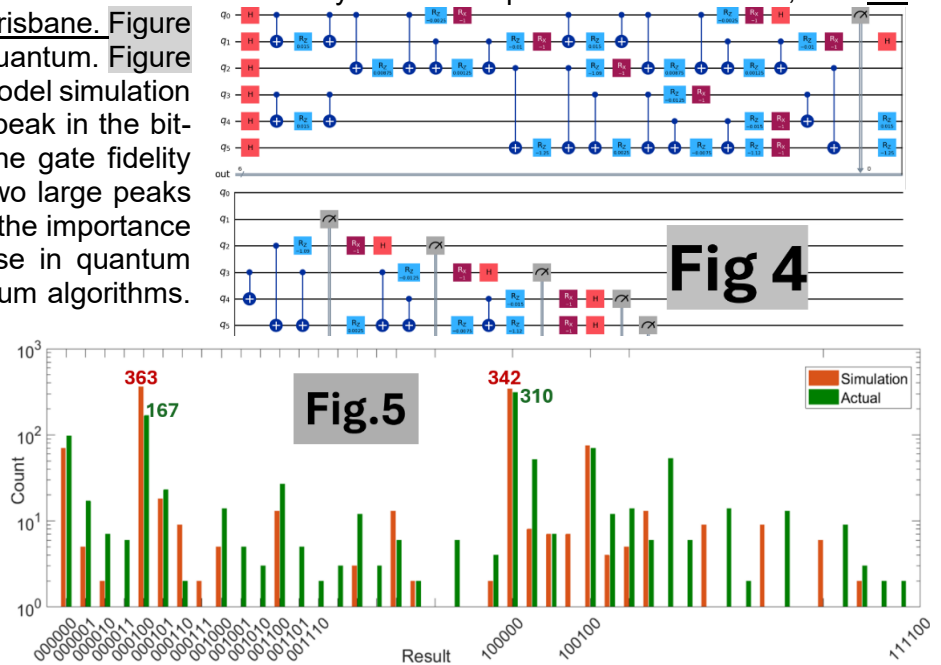
Fig.2



Key Results: Quantum Circuit model: Results were achieved by simulated quantum circuit model, and the real quantum computer, IBM Quantum, Brisbane. Figure 4 shows the QAOA circuit used in IBM Quantum. Figure 5 presents the expected result from the model simulation on IBM Quantum, which shows a large peak in the bit-string 000100. In the real QC results, the gate fidelity appears to be rather poor, resulting in two large peaks one on bit-string 000100. This highlights the importance of coherence states and controlled noise in quantum systems for the implementation of quantum algorithms.

Annealing model: Using the simulated D-Wave machines working on a local PC, the IBM quantum result was validated where the ground state was found to be $\{x_{00}, x_{01}, x_{02}, x_{10}, x_{11}, x_{12}\} = \{0, 0, 0, 1, 0, 0\}$.

References: [1] Pakela et al., DOI 10.1002/mp.13840 [2] Nazareth et al., DOI 10.1088/0031-9155/60/10/4137



Title

Pleckstrin Homology domains regulate PI3K/Akt to block breast cancer dissemination

Authors

Matthew Eason ^{1,2}, Anindya Sen ^{3,4}, Se Jong Lee, PhD ^{3,4}, Musavvir Mahmud ^{2,5,6,7}, Poornima Dubey, PhD ^{2,5,6,7}, Talia Guardia, PhD ^{1,2}, Anthony Kim, PhD ^{2,5,6,7}, Nathan Wright, PhD ⁸, Konstantinos Konstantopoulos, PhD ^{3,4}, and Aikaterini Kontrogianni-Konstantopoulos, PhD ^{1,2}

Author Affiliations

1. Department of Biochemistry and Molecular Biology, University of Maryland School of Medicine, Baltimore, MD 21201.
2. Marlene and Stewart Greenebaum Comprehensive Cancer Center, Baltimore, MD 21201.
3. Department of Chemical and Biomolecular Engineering, The Johns Hopkins University, Baltimore, MD 21218.
4. Institute for NanoBioTechnology, Johns Hopkins University, Baltimore, MD 21218.
5. Department of Neurosurgery, University of Maryland School of Medicine, Baltimore, Maryland 21201, United States.
6. Department of Pharmacology, University of Maryland School of Medicine, Baltimore, Maryland 21201, United States.
7. Department of Pharmaceutical Sciences, University of Maryland School of Pharmacy, Baltimore, Maryland 21201, United States.
8. Department of Chemistry and Biochemistry, James Madison University, Harrisonburg, Virginia, USA

Abstract

Current cancer therapies target tumor proliferation and survival but fail to target metastatic dissemination. Obscurin, a giant signaling protein that localizes to the breast epithelial cell membrane, is a metastasis suppressor and is commonly lost in breast cancer. Obscurin loss upregulates PI3K/Akt which is altered in 30-40% of invasive breast carcinomas. The obscurin-pleckstrin homology (PH) domain interacts with the PI3K-p85 regulatory subunit. Here, we demonstrate that ectopic expression of membrane-targeted obscurin-PH domain in aggressive breast cancer cells, via use of adenovirus or lipid nanoparticles, sequesters p85, suppressing PI3K/Akt activity. p85 sequestration eliminates filopodia, hampering migration and adhesion to pre-metastatic niche extracellular matrix substrates. This intervention also eradicates invadopodia, and reduces matrix metalloproteinase expression, blocking invasion and dissemination. We recapitulate this phenotype using the structurally homologous kalirin and PLC γ 1 PH-domains, and ultimately uncover, via *in silico* mutagenesis analysis coupled with stimulated emission depletion microscopy, a family of 9 PH-domains as p85-regulators, pinpointing the p85 inhibition dissemination suppressor (PIDS) motif that mediates this effect. As PI3K inhibitors targeting the p110 catalytic subunit are limited to metastatic hormone receptor positive breast cancer, this work uncovers a new class of PI3K inhibitors in the form of the PH-domain, targeting the p85 regulatory subunit and setting the pace for the design of a novel therapy to combat metastatic breast cancer.

Prediction of metastasis-free survival in patients with prostate adenocarcinoma using primary tumor and lymph node radiomics from pre-treatment PSMA PET/CT scans.

Apurva Singh, PhD, William Silva Mendes, MD, Sangbo Oh, MD, Ozan Cem Guler, MD, Phuoc Tran, MD, PhD, Cem Onal, MD, Lei Ren, PhD

Purpose: To predict metastasis-free survival (MFS) for patients with prostate adenocarcinoma treated with androgen deprivation therapy and external radiotherapy using clinical factors and radiomics extracted from pre-treatment PSMA PET/CT scans.

Method: Our cohort includes 134 prostate adenocarcinoma patients (60 patients having nodal involvement). Gross-tumor-volumes of primary tumor (GTVp) and nodes (GTVn) on CT, PET scans were segmented. Features were extracted and Z-score-normalized; dimensionality reduction performed using Principal-Components-Analysis. For patients with only primary tumor, we took three principal-components (PCs) from CT and PET, respectively. For patients with nodes, we calculated weighted-average (by volume) of radiomics from primary tumor and nodes, computed their first PC, combined with two PCs from GTVp to obtain three PCs from CT and PET, respectively. Radiomics PCs and clinical variables (age, Gleason score, virgin-prostate-specific-antigen (vPSA), PSA_relapse) formed the predictors. Due to imbalance in MFS data (metastasis-24, no metastasis-110), we performed 70:30 train-test split and applied imbalance correction to training data. Univariate Cox-regression was used to select top five predictors (logistic regression $p < 0.05$) for model 1. Multivariate Cox-regression analysis was performed on imbalance-corrected train data and fit on test data (using predictors selected from train data). Model 2 was built using clinical variables, radiomic PCs from primary tumors to assess improvement by adding node-radiomics.

Results: Results of time-to-event analysis (metastasis-free survival) were- Cox-regression c-scores: model1: train- 0.70 [0.64, 0.71]; test- 0.61 [0.56, 0.62]; model2: train- 0.67 [0.62, 0.68]; test- 0.58 [0.54, 0.59]. We observed that integration of node with primary tumor-radiomics improved performance of the prognostic model.

Conclusion: This is one of the first studies to explore the prognostic value of pre-treatment PSMA-PET, a relatively recent advancement in the care of prostate adenocarcinoma patients. Results showed that using PSMA PET/CT radiomics information from primary tumor and nodes improves MFS prediction, compared to using primary tumor-radiomics only.

Centering Black Voices: Factors Influencing a Cancer Patient's Decision to Join a Clinical Trial

Charlyn Gomez, BS¹; Kaysee Baker, MS²; Caitlin Eggleston, BS²; Matthew Ferris, MD²; Jason Molitoris, MD, PhD²; Akshar Patel, MD²; Zaker Hamid Rana, MD²; Sarah McAvoy, MD²; Elizabeth Nichols, MD²; William Regine, MD, FACR, FACRO²; Søren M. Bentzen PhD, DMSca^{2,3}; Melissa Ana Liriano Vyfhuis, MD, PhD²

1. University of Maryland School of Medicine, Baltimore, MD
2. Department of Radiation Oncology, University of Maryland School of Medicine, Baltimore, MD
3. Department of Epidemiology and Public Health, Biostatistics and Bioinformatics Division, University of Maryland School of Medicine, Baltimore, Maryland

ABSTRACT

Purpose: There has been a recent decline in Black participant (BP) enrollment in cancer-related clinical trials and the etiology remains poorly understood. We aim to characterize psychosocial factors that patients with curative gastrointestinal, thoracic, gynecological, and head and neck malignancies consider when enrolling in a research study, with the goal of improved recruitment of Black patients.

Methods and Materials: We conducted a cross-sectional, descriptive study using a questionnaire adapted from two previously validated surveys to patients who completed definitive radiation treatment for the aforementioned malignancies. Chi-square tests and Mann-Whitney U test were used to assess associations or differences between the populations.

Results: From October 2023 to February 2024, 247 eligible patients were asked to participate, and 172 patients agreed (compliance 70%). BP comprised 28.2% of the patient population (n=69), were predominantly women (46%vs. 60.9%; p=0.037), were less likely to be married (23.2%vs.63.6%; p<.001), have a Bachelor's degree (5.8%vs.17.6%; p=.019), and have a lower median income (\$73,023vs.\$107,542; p<0.001) when compared to non-Black patients (NBP). Both groups were equally asked to participate in a clinical trial (BPvs.NBP; 17.2%vs.21.5%; p=NS). BP were more apt to agree with statements that illness/death is determined by God's

will, (48%vs.17.3%; $p=0.024$) and that God determines wellness, not research (55.1%vs.16.5%; $p<0.001$) when compared to NBP. Eighteen percent of BP agreed that research harms minorities vs. 3.6% of NBP ($p=.001$). BP felt that there was nothing for them (11.8%vs.3.2%; $p=0.01$) or their community (25.1%vs.5.3%; $p=0.006$) to gain by participating in research when compared to the NBP. $\geq 90\%$ of both groups agreed that they trust their cancer doctors.

Conclusions: Our data suggests the importance of spiritual themes within the Black community when considering clinical trials. Though most patients trust their cancer care team, there remains underlying distrust in clinical research among Black patients.

Clinical Toxicity Profiles of Neoadjuvant Volumetric Modulated Arc Radiotherapy and Proton Beam Radiotherapy for Soft Tissue Sarcoma: A Single-Institution Retrospective Analysis

Alexander Allen, Kai Sun, Adeniyi Olabumuyi, Zachery Keepers, Sarayu Valluri, Hurley Ryan, Hua-Ren Cherng, Soren Bentzen, Michael Kim, Dan Kunaprayoon, William Regine

Purpose/Objective(s): Since the advent of limb-sparing surgery for soft tissue sarcoma (STS), treatment goals for this malignancy have focused on reducing toxicities that impair patient quality of life while maintaining a high rate of local control. In the treatment of STS, proton beam radiotherapy (PBT) can better spare adjacent soft tissue and bone due to superior dose-fall off compared to photon-based modalities such as volumetric modulated arc therapy (VMAT). While there is evidence documenting the dosimetric advantages of PBT, there is sparse literature assessing whether these advantages translate into clinical benefits. We hypothesized that, for patients with STS receiving neoadjuvant radiotherapy (RT) followed by resection, the use of PBT would be associated with a lower rate of physician-reported fibrosis, edema, and joint stiffness of the treated extremity compared to VMAT.

Materials/Methods: We performed a retrospective review of patients with STS who received neoadjuvant VMAT or PBT between 1/1/2012 and 6/1/2024 within a single health system prior to surgical resection. Patients undergoing re-irradiation, patients who received 3DCRT or electron neoadjuvant RT, and patients who did not undergo resection after RT, were excluded. A Fine-Gray model was used to compare the cumulative incidences of physician-reported toxicities between treatment groups (with adjustment for death as a competing risk factor) by generating a subdistribution hazard ratio (SHR).

Results: The analysis included 80 patients, of whom 47.5% (38/80) received VMAT and 52.5% (42/80) received PBT. Median age was 60 years [48.8 – 69.8] and median follow-up time was 29 months [16.5–52.8]. There were no statistically significant inter-group differences for the following variables: ECOG status, initial tumor size (median 10.1 cm [6.9-13.2]), distance from tumor to nearest joint (median 5 cm [2.2–11.2]), upper or lower extremity location of tumor, radiation dose (median 50.4 Gy [50-50.4]), days spent in hospital for tumor resection, or need for flap or reconstruction. There was no difference in acute post-operative wound complications between the two modalities ($p=0.446$). Compared to VMAT, PBT was associated with a decreased cumulative incidence of joint stiffness (SHR 0.611 [CI 0.452 – 0.852] $p=0.001$) and joint fibrosis (SHR 0.584 [CI 0.434–0.786] $p=0.0001$). PBT was associated with a decreased cumulative incidence of extremity edema, however, this was not statistically significant (SHR 0.849 [CI 0.693 – 1.04] $p=0.112$). Overall local control was 88.8% and there was no difference in local failure between the two modalities ($p=0.141$).

Conclusion: This retrospective data shows that, in the treatment of STS with neoadjuvant RT, PBT is associated with decreased physician-reported rates of joint fibrosis and stiffness of the treated extremity when compared to VMAT. These findings suggest that a prospective clinical trial is warranted to definitively compare the toxicity profiles of these two radiation modalities.